UC Santa Barbara
UC Santa Barbara Electronic Theses and Dissertations

Title

ADCN: An Anisotropic Density-Based Clustering Algorithm for Discovering Spatial Point Patterns with Noise

Permalink

https://escholarship.org/uc/item/3np9r4zb

Author

Mai, Gengchen

Publication Date

2017

Peer reviewed|Thesis/dissertation

eScholarship.org Powered by the California Digital Library
University of California

University of California
Santa Barbara

ADCN: An Anisotropic Density-Based Clustering Algorithm for Discovering Spatial Point Patterns with Noise

A dissertation submitted in partial satisfaction
of the requirements for the degree

Master of Art
in
Geography

by

Gengchen Mai

Committee in charge:

Professor Krzysztof Janowicz, Chair
Professor Werner Kuhn
Professor Kostas Goulias

January 2018

The Dissertation of Gengchen Mai is approved.

Professor Werner Kuhn

Professor Kostas Goulias

Professor Krzysztof Janowicz, Committee Chair

June 2017

ADCN: An Anisotropic Density-Based Clustering Algorithm for Discovering Spatial Point Patterns with Noise

Copyright © 2018

by

Gengchen Mai

Acknowledgements

I would like to thank the members of my Master's committee for their great suggestions and guidance throughout this thesis. I would like to thank my adviser, Professor Krzysztof (Jano) Janowicz, for his very strong support during every stage of my life as a graduate student. The last two years have been very difficult for me. The loss of family members nearly put me in a hole while Jano and other members from STKO Lab helped me to get through this extremely difficult time. Nonetheless, these two years make me become very enthusiastic about research and it is Jano who makes me an independent researcher. I would like to thank Yingjie Hu and Song Gao for helping me build up the research framework of this thesis and offering me many useful suggestions. I would like to thank all of my STKO colleagues for their companionship and friendship. I would like to thank Professor Daniel Montello and Professor Martin Raubal for inspiring me during the initial stage of this research. Last, but most importantly, I would like to thank my family, especially my mother, for their unconditional love, support and companion during the darker times of my life.

Curriculum Vitæ
Gengchen Mai

Education

2020	Ph.D. in Geography (Expected), University of California, Santa Barbara.
2017	M.A. in Geography (Expected), University of California, Santa Barbara.
2015	B.S. in Geographic Information System, Wuhan University.

Awards

- **Travel Grants**

2017 The Jack & Laura Dangermond Travel Scholarship for ACM SIGSPATIAL 2017

2017 The Jack & Laura Dangermond Travel Scholarship for AAG 2017

2016 The Jack & Laura Dangermond Travel Scholarship for ACM SIGSPATIAL 2016

2016 The Jack & Laura Dangermond Travel Scholarship for GIScience 2016

2016 NSF Student Fellowship for RW2016

2016 The Jack & Laura Dangermond Travel Scholarship for RW2016

2016 The Jack & Laura Dangermond Travel Scholarship for AAG 2016

- **Fellowships, Scholarships, and Awards**

2017 The 1st Place Best Paper Award at AAG 2017 GIS Special Group Student Paper Competition for "*Beyond Coordinates: Incorporating Geographic Knowledge into Geocoding Services Using Linked Open Data*" (co-author)

2015 UCSB Geography Doctoral Scholars Fellowship

2015 Outstanding Undergraduate of Wuhan University

2013 China National Fellowship

2013 First-class scholarship and Merit Student of School of Resource and Environmental Sciences, Wuhan University

2012 China National Fellowship

2012 First-class scholarship and Merit Student of School of Resource and Environmental Sciences, Wuhan University

2011 China National Fellowship

2011 First-class scholarship and Merit Student of School of Resource and Environmental Sciences, Wuhan University

Publications

- **Book Chapters**

1. Song Gao, **Gengchen Mai**. (2017) Mobile GIS and Location-Based Services. In Bo Huang, Thomas J. Cova, and Ming-Hsiang Tsou et al.(Eds): *Comprehensive Geographic Information Systems*, Elsevier. Oxford, UK.

- **Peer-reviewed Journal Articles**

1. **Gengchen Mai**, Krzysztof Janowicz, Yingjie Hu, Song Gao. ADCN: An Anisotropic Density-Based Clustering Algorithm for Discovering Spatial Point Patterns with Noise. *Transactions in GIS*, in press. `DOI:10.1111/tgis.12313`
2. Shiliang Su, Yaping Wang, Fanghan Luo, **Gengchen Mai**, Jian Pu. Peri-urban vegetated landscape pattern changes in relation to socioeconomic development. *Ecological Indicators* 46 (2014) 477486.
3. Shiliang Su, Yina Hu, Fanghan Luo, **Gengchen Mai**, Yaping Wang. Farmland fragmentation due to anthropogenic activity in rapidly developing region. *Agricultural Systems* 131 (2014) 8793.
4. Rui Xiao, Shiliang Su, **Gengchen Mai**, Zhonghao Zhang, Chenxue Yang. Quantifying determinants of cash crop expansion and their relative effects using logistic regression modeling and variance partitioning. *International Journal of Applied Earth Observation and Geoinformation* 34 (2015) 258263.

- **Conference Papers**

1. Bo Yan, Krzysztof Janowicz, **Gengchen Mai**, Song Gao. From ITDL to Place2Vec - Reasoning About Place Type Similarity and Relatedness by Learning Embeddings From Augmented Spatial Contexts, In: *Proceedings of the 25th International Conference on Advances in Geographic Information Systems (ACM SIGSPATIAL 2017)*, November 7 - 10, 2017, Redondo Beach, California, USA. (Full paper accepted)
2. Blake Regalia, Krzysztof Janowicz, **Gengchen Mai**. Phuzzy.link: A SPARQL-powered Client-Sided Extensible Semantic Web Browser, In: *Proceedings of 3rd International Workshop on Visualization and Interaction for Ontologies and Linked Data (VOILA 2017) co-located with ISWC 2017*, October 22, 2017, Vienna, Austria. (Full paper accepted)

3. **Gengchen Mai**, Krzysztof Janowicz, Yingjie Hu, Song Gao. ADCN: An Anisotropic Density-Based Clustering Algorithm, In: *Proceedings of the 24th International Conference on Advances in Geographic Information Systems (ACM SIGSPATIAL 2016)*, October 31 - November 3, 2016, San Francisco Bay Area, California, USA. (Short paper accepted)
4. **Gengchen Mai**, Krzysztof Janowicz, Yingjie Hu, Grant McKenzie. A Linked Data Driven Visual Interface for the Multi-Perspective Exploration of Data Across Repositories, In: *Proceedings of 2nd International Workshop on Visualization and Interaction for Ontologies and Linked Data (VOILA 2016) co-located with ISWC 2016*, October 17, 2016, Kobe, Japan. (Full paper accepted)
5. Song Gao, Rui Zhu, **Gengchen Mai**. Identifying Local Spatiotemporal Autocorrelation Patterns of Taxi Pick-ups and Drop-offs, In: *Proceedings of the 9th International Conference on Geographic Information Science*, September 27 - 30, 2016, Montreal, Canada. (Short paper accepted)
6. Krzysztof Janowicz, Yingjie Hu, Grant McKenzie, Song Gao, Blake Regalia, **Gengchen Mai**, Rui Zhu, Benjamin Adams, and Kerry Taylor. Moon Landing or Safari? A Study of Systematic Errors and Their Causes in Geographic Linked Data, In: *Proceedings of the 9th International Conference on Geographic Information Science*, September 27 - 30, 2016, Montreal, Canada. (Full paper accepted)

Abstract

ADCN: An Anisotropic Density-Based Clustering Algorithm for Discovering Spatial Point Patterns with Noise

by

Gengchen Mai

Density-based clustering algorithms such as DBSCAN have been widely used for spatial knowledge discovery as they offer several key advantages compared to other clustering algorithms. They can discover clusters with arbitrary shapes, are robust to noise and do not require prior knowledge (or estimation) of the number of clusters. The idea of using a scan circle centered at each point with a search radius *Eps* to find at least *MinPts* points as a criterion for deriving local density is easily understandable and sufficient for exploring isotropic spatial point patterns. However, there are many cases that cannot be adequately captured this way, particularly if they involve linear features or shapes with a continuously changing density such as a spiral. In such cases, DBSCAN tends to either create an increasing number of small clusters or add noise points into large clusters. Therefore, in this paper, we propose a novel anisotropic density-based clustering algorithm (ADCN). To motivate our work, we introduce synthetic and real-world cases that cannot be sufficiently handled by DBSCAN (and OPTICS). We then present our clustering algorithm and test it with a wide range of cases. We demonstrate that our algorithm can perform as equally well as DBSCAN in cases that do not explicitly benefit from an anisotropic perspective and that it outperforms DBSCAN in cases that do. We show that our approach has the same time complexity as DBSCAN and OPTICS, namely O(n log n) when using a spatial index and O(n^2) otherwise. We provide an implementation and test the runtime over multiple cases. Finally, we apply DBSCAN, OPTICS, and

ADCN to the task of extracting urban areas of interest (AOI) from geotagged photos in six cities. Visual comparison shows that, comparing to DBSCAN and OPTICS, ADCN is inclined to extract AOIs with linear shapes which follow the underline road networks. ADCN also turns out to connect clusters when the spatial distribution of them shows similar directions.

Contents

Curriculum Vitae **v**

Abstract **viii**

1 Introduction and Motivation **1**

2 Related Work **6**
- 2.1 Density-based Clustering Algorithm . . . 7
- 2.2 Anisotropicity . . . 8
- 2.3 Clustering Comparison Indexes . . . 11
- 2.4 Research Question . . . 16

3 Anisotropic Density-based Clustering with Noise (ADCN) **17**
- 3.1 Anisotropic Perspective on Local Density . . . 17
- 3.2 Anisotropic Density-Based Clusters . . . 19
- 3.3 ADCN Algorithms . . . 24

4 Experiments and Performance Evaluation **29**
- 4.1 Experiment Designs . . . 30
- 4.2 Test Environment . . . 31
- 4.3 Evaluation of Clustering Quality . . . 35
- 4.4 Evaluation of Clustering Efficiency . . . 38

5 Real World Application **44**
- 5.1 Data Preprocessing and Clustering . . . 45
- 5.2 Constructing AOI from point clusters using chi-shape algorithm . . . 46

6 Conclusion and Future Work **56**
- 6.1 Conclusion . . . 56
- 6.2 Future Work . . . 58

Bibliography **60**

Chapter 1

Introduction and Motivation

Cluster analysis is a key component of modern knowledge discovery whose objective is to maximize the intra-cluster similarity while minimizing the inter-cluster similarity at the same time. The objects as a basic analytic unit can be anything whose attributes can be quantified, including geographic footprints from social media platforms [1, 2, 3, 4], human activity traces [5], places, documents [6, 7], and so on. Because of the domain independent definition of "objects" in cluster analysis, it has been widely applied to data analysis tasks from many research disciplines and is widely considered a key technique used for reducing dimensionality, identifying prototypes, cleansing noise, determining core regions, and segmentation.

A wide range of clustering algorithms have been proposed and implemented over the last decades to achieve the objective of clustering analysis from different perspectives. Common examples include DBSCAN [8], OPTICS [9], K-means [10], K-medians [11], ASCDT [12], and Mean Shift [13]. These techniques often yield different clustering results for the same data due to differences in the underlying understanding of what should be clustered and how. K-means and K-medians, for instance, first find representatives for each cluster and update them as well as the cluster memberships of each object by minimizing the distance between cluster representatives and other objects in the same cluster. Hence, detected clusters will have spherical shapes with similar sizes. Both techniques also have no notion of *noise* as each object belongs to some cluster. In contrast, DBSCAN, OPTICS or other density-based clustering algorithms try to find clusters in which the density of objects is larger than a threshold. The resulting clusters can have arbitrary shapes and varied sizes but with similar or homogenous object densities. Noise is defined as objects in low density regions. Delaunay triangulation-based clustering algorithms, like ASCDT [12], find clusters based on spatial proximity between objects defined via Delaunay triangulations. due to different distance metrics (Delaunay triangulation based distance metrics), ASCDT can discover clusters of complicated shapes and non-homogeneous densities in a spatial database. However, Delaunay triangulation based clustering algorithms cannot be easily scaled up to a large spatial dataset because of the high time complexity for computing the triangulation.

Many clustering algorithms including all algorithms we discussed above depend on *distance* as their main criterion [14]. They assume *isotropic* second-order effects (i.e., spatial dependence) among spatial objects thereby implying that the magnitude of similarity and interaction between two objects mostly depends on their distance. However, the genesis of many geographic phenomena demonstrates clear *anisotropic* spatial processes. As for ecological and geological features, such as the spatial distribution of rocks [15], soil [16], and airborne pollution [17], their spatial patterns vary in direction [18]. Similarly, data about urban dynamics from social media, the census, transportation studies, and so forth, are highly restricted and defined by the layout of urban spaces, and thus show clear variance along directions. To give a concrete example, geo-tagged images be it in the city or the great outdoors, show clear directional patterns due to roads, hiking trails, or simply for the fact that they originate from human, goal-directed trajectories. Isotropic clustering algorithms such as DBSCAN have difficulties dealing with the resulting point patterns and either fail to eliminate noise or do so at the expense of introducing many small clusters. One such example is depicted in Figure 1.1. Due to the changing density, algorithms such as DBSCAN will classify some noise, i.e., points between the spiral arms, as being part of the cluster. To address this problem, we propose an anisotropic density-based clustering algorithm.

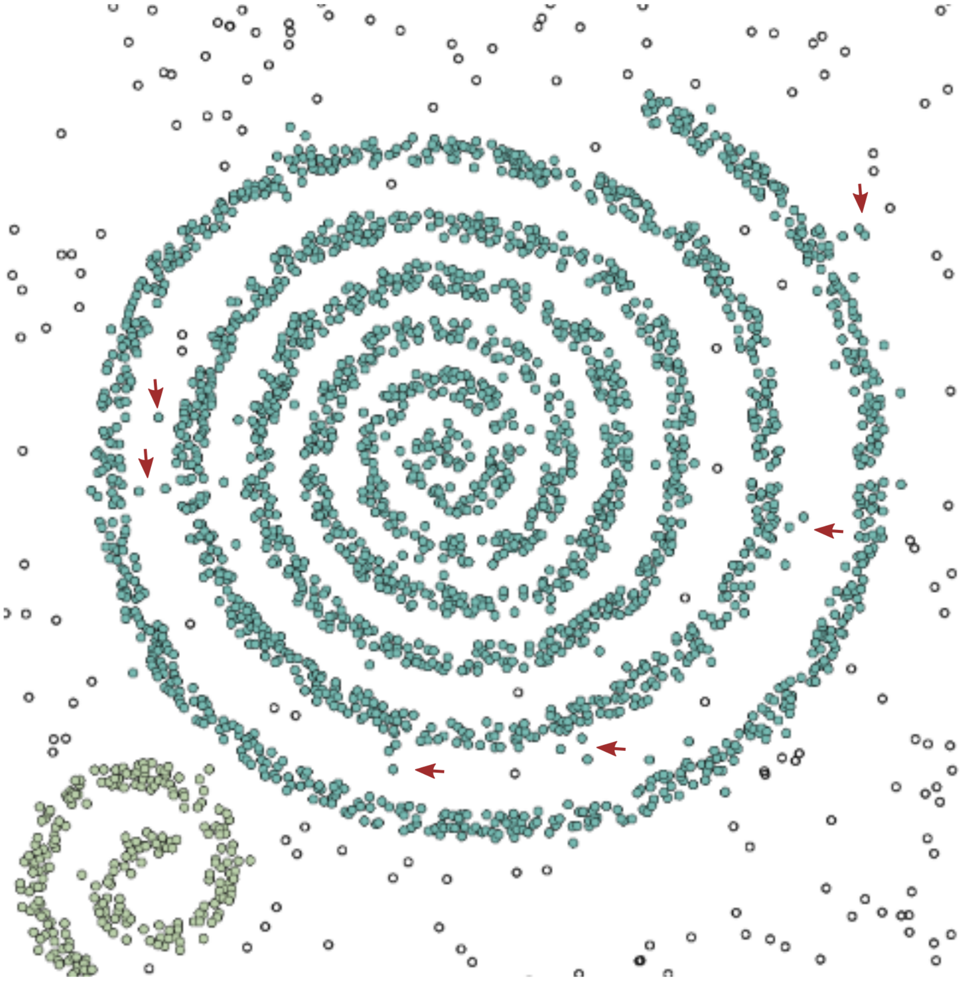

Figure 1.1: A spiral pattern clustered using DBSCAN. Some noise points are indicated by red arrows.

More specifically, the research contributions of this paper are as follows:

- We introduce an anisotropic density-based clustering algorithm (ADCN [1]). While

---

[1] This paper is based on the short paper [19] and the paper [20]. It also adds an open source imple-

the algorithm differs in the underlying assumptions, it uses the same two parameters as DBSCAN, namely *Eps* and *MinPts*, thereby providing an intuitive explanation and integration into existing workflows.

- We motivate the need for such algorithm by showing 12 synthetic and 8 real-world use cases and each with 3 different noise definitions modeled as buffers that generate a total of 60 test cases.
- We demonstrate that ADCN performs as well as DBSCAN (and OPTICS) for isotropic cases but outperforms both algorithms in cases that benefit from an anisotropic perspective.
- We argue that ADCN has the same time complexity as DBSCAN and OPTICS, namely O(n log n) when using a spatial index and O(n^2) otherwise.
- We provide an implementation for ADCN and apply it to the use cases to demonstrate the runtime behavior of our algorithm. As ADCN has to compute whether a point is within an ellipse instead of merely relying on the radius of the scan circle, its runtime is slower than DBSCAN while remaining comparable to OPTICS. We discuss how the runtime difference can be reduced by using a spatial index and by testing the radius case first.
- Finally, we apply ADCN, DBSCAN, and OPTICS to a 2013-2014 Flickr geotagged photo dataset from six cities to extract urban areas of interest (AOI). Although there is no *ground truth* in this task, by comparing the extracted AOIs from different algorithms, we are able to show that the AOIs extracted from ADCN tend to have linear shapes that follow road networks. We perform this analysis to show that

---

mentation of ADCN, a test environment, as well as new evaluation results on a larger sample.

ADCN does not only yield different results for test cases but that these differences have impact on cluster formation using large scale real-world data.

The remainder of the paper is structured as follows. First, in Chapter 2, we discuss related work including variants of DBSCAN, anisotropicity of spatial point patterns, and clustering comparison indexes. Next, we introduce ADCN and discuss two potential realizations of measuring anisotropicity in Chapter 3. In Chapter 4, several experiments are described to demonstrate the effectiveness of ADCN. Use cases, the development of a test environment, and a performance evaluation of ADCN are presented in Chapter 4. Next, in Chapter 5, ADCN, DBSCAN and OPTICS are applied to a real-world application, namely urban AOI extraction, to show the advantages of ADCN. Finally, in Chapter 6, we conclude our work and point to directions for future work.

Chapter 2

Related Work

Clustering algorithms can be classified into several categories, including but not limited to partitioning, hierarchical, density-based, graph-based, and grid-based approaches [21, 12]. Each of these categories contains several well known clustering algorithms with their specific pros and cons. Partitioning clustering, such as K-Means, PAM [22] and CLARANS [23], aims at finding mutually exclusive clusters of spherical shapes. It has difficulties in handling clusters of different sizes and shapes. Hierarchical clustering, such as single-link and complete-link, approaches build a hierarchical tree of clusters. When there are some erroneous merges or splits during the hierarchical tree construction process, they cannot be corrected later. Grid-based clustering segments the data space into grid cells [24]. That means it will suffer from the common drawbacks of image operations. Here we focus on the density-based approaches and we will review them below.

2.1 Density-based Clustering Algorithm

Density-based clustering algorithms are widely used in big geo-data mining and analysis tasks, like generating polygons from a set of points [25, 26, 27], discovering urban areas of interest [2], revealing vague cognitive regions [3], detecting human mobility patterns [28, 29, 30, 31], and identifying animal mobility patterns [32].

Density-based clustering algorithms, such as DBSCAN [8], OPTICS [9], DENCLUE [33], have many advantages over other approaches. Figure 2.1 shows the best clustering results from K-Means and DBSCAN based on one clustering result comparison index [1]. By comparing the clustering results between these two algorithms, we can observe several advantages of DBSCAN including: 1) the ability to discover clusters with arbitrary shapes; 2) robustness to noise; and 3) no requirement to pre-define the number of clusters. While DBSCAN remains the most popular density-based clustering method, many related algorithms have been proposed to compensate for some of its limitations. Most of them, such as OPTICS [9] and VDBSCAN [34], address problems arising from density variations within clusters. Others, such as ST-DBSCAN [35], add a temporal dimension which means the objects within each extracted cluster are approximated to each other spatio-temporally. However, an additional temporal parameter is necessary. GDBSCAN [36] extends DBSCAN to include non-spatial attributes into clustering and enables the clustering of high dimensional data. NET-DBSCAN [37] revises DBSCAN for network data by redefining the distance matrics based on network structures. To improve the computational efficiency, algorithms such as IDBSCAN [38] and KIDBSCAN [24] have been proposed.

---

[1] Here we use Normalized Mutual Information index which we will discuss in Section 4.

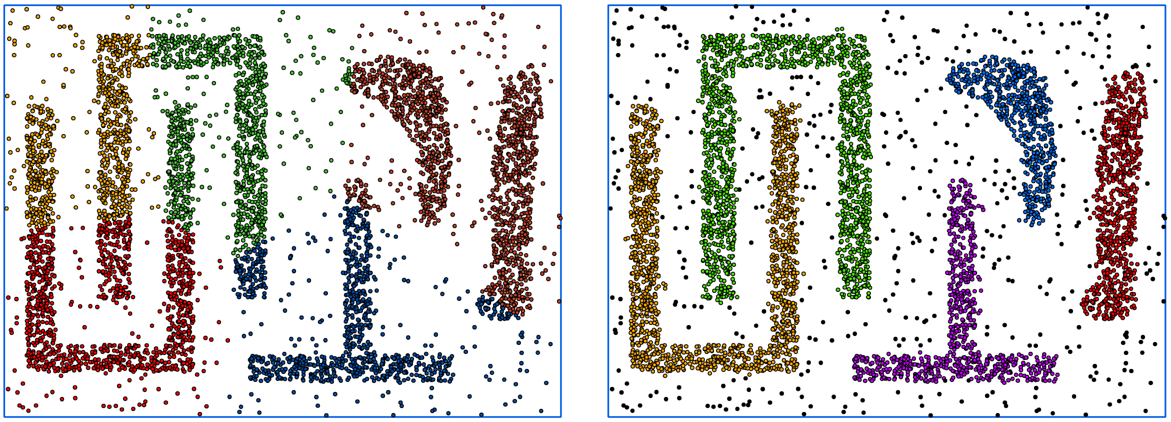

(a) K-Means (b) DBSCAN

Figure 2.1: Clustering result comparison between K-means and DBSCAN.

2.2 Anisotropicity

All of these algorithms use distance as the major clustering criterion. They assume that the observed spatial patterns are isotropic, i.e., that intensity dose not vary by direction. For example, DBSCAN uses a scan circle with an *Eps* radius centered at each point to evaluate the local density around the corresponding point. A cluster is created and expanded as long as the number of points inside this circle (*Eps*-neigborhood) is larger than *MinPts*. Consequently, DBSCAN does not consider the spatial distribution of the *Eps*-neigborhood which poses problems for linear patterns.

Some clustering algorithms do consider local directions. However, most of these so-call direction-based clustering techniques use spatial data which have a pre-defined local direction, e.g., trajectory data. The *local direction* of one point is pre-defined as the direction of the vector which is part of the trajectories with the corresponding point as its origination or destination. DEN [39] is one direction-based clustering method which uses a grid data structure to group trajectories by moving directions. PDC+ [40] is another trajectory specific DBSCAN variant that includes the direction per point. DB-

SMoT [41] includes both the direction and temporal information of GPS trajectories from fishing vessel into the clustering process. Although all of these three direction-based clustering algorithms incorporate local direction as one of the clustering criteria, they can be applied to only trajectories data.

Many spatial data sets do not have predefined local direction information which can show the moving directions of objects under study. However, because the underline spatial point process is anisotropic, the spatial patterns shown by the cumulative spatial datasets generated from this process varies in direction and demonstrates the direction information of underline spatial point process. For example, geotagged social media data, like Foursquare check-in data, geotagged tweets, reflects human dynamic mobilities in/across the urban area which are highly restricted by the urban spatial structure (road networks). So these user-generated geospatial data show a spatial pattern distributed along road networks. Figure 2.2 shows the spatial distribution of geotagged tweets during April 2014 in California, USA. The major road networks in California is clearly revealed from these tweets.

Anisotropicity [18] describes the variation of directions in spatial point processes in contrast to *isotropicity*. It is another way to describe intensity variation in spatial point process other than first- and second-order effects. *Anisotropicity* has been studied in the context of interpolation where a spatially continuous phenomenon is measured, such as directional variogram [17] and different modifications of Kriging methods based on local anisotropicity [42, 43, 44]. In this work we focus on *anisotropicity* of spatial point processes. Researchers studied *anisotropicity* of spatial point processes from a theoretical perspective by analyzing their realizations such as detecting anisotropy in spatial point patterns [45] and estimating geometric anisotropic spatial point patterns [46, 47]. Here, we study *anisotropicity* in the context of density-based clustering algorithms.

A few clustering algorithms take anisotropic processes into account. For instance,

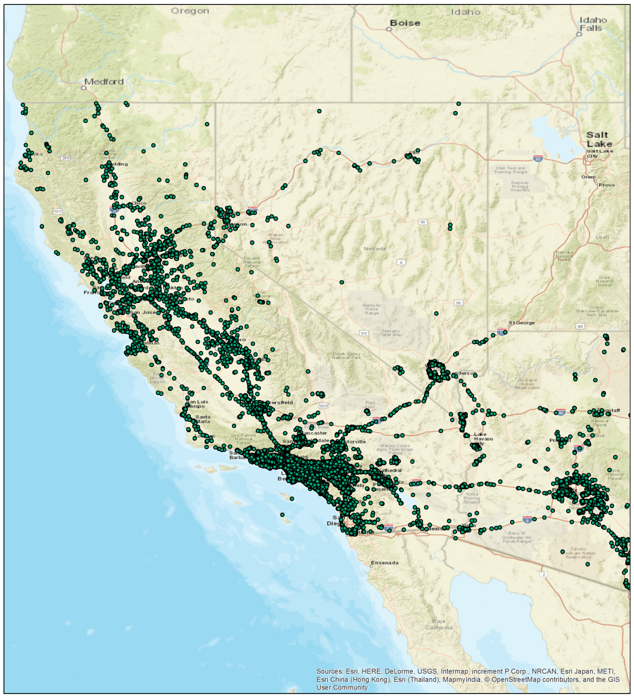

Sources: Esri, HERE, DeLorme, USGS, Intermap, increment P Corp., NRCAN, Esri Japan, METI, Esri China (Hong Kong), Esri (Thailand), MapmyIndia, © OpenStreetMap contributors, and the GIS User Community

Figure 2.2: Geo-tagged tweets during April, 2014 in California, USA

in order to obtain good results for crack detection, an anisotropic clustering algorithm [48] has been proposed to revise DBSCAN by changing the distance metric to geodesic distance. QUAC [49] demonstrates another anisotropic clustering algorithm which does not make an isotropic assumption. It takes the advantages of anisotropic Gaussian kernels to adapt to local data shapes and scales and prevents singularities from occurring by fitting the Gaussian mixture model (GMM). QUAC emphasizes the limitation of an isotropic assumption and highlights the power of anisotropic clustering. However, due to the use of anisotropic Gaussian kernels, QUAC can only detect clusters which have ellipsoid shapes. Each cluster derived from QUAC will have a major direction. In real-world cases, spatial pattern will show arbitrary shapes. Even more, the local direction is not necessary the same between and even within clusters. Instead, it is reasonable to assume that local direction can change continuously in different parts of the same cluster.

From the above discussion of different clustering algorithms, it is clear that an isotropic assumption may be inappropriate for many geographic phenomena. On top of local density, it is necessary to consider local direction during the clustering process. This local direction is not necessary the same for one cluster. Instead, it is reasonable that the local direction is changing continuously in different parts of one cluster.

2.3 Clustering Comparison Indexes

Evaluating the clustering result is the final and important step in cluster analysis. In general, clustering evaluation methods can be divided into two categories: intrinsic and extrinsic [50]. Given a similarity metric between objects, intrinsic clustering evaluation methods compute how similar objects in one cluster are to each other, and how dissimilar to objects from different clusters they are. In other words, intrinsic evaluation assesses the goodness of a clustering by computing how well the clusters are separated [21]. When a *ground truth/gold standard* is available, extrinsic clustering evaluation methods will play a role by comparing the output from one clustering algorithm to the *ground truth*. Here, *ground truth/gold standard* is the ideal clustering result obtained from human experts, prior knowledge, convention, or otherwise. In this work, we focus on extrinsic methods.

Many clustering comparison indexes have been proposed for extrinsic clustering evaluation. Marina et al. [51], Nguyen Xuan et al. [52], and more recent Jiawei et al. [21] have presented a review of these clustering comparison indexes. Traditionally, many researchers agree that measures for comparing clusterings can be classified as *pair-counting based measures*, *set-matching based measures*, and *information theoretic measures*. But recently, new measures have been proposed which cannot be classified into these three categories, such as clustering measure using *density profile* [53], *Mallows distance based measures* [54], and *transportation distance based measure* [55]. We will briefly discuss them below.

Pair-counting based measures count pairs of items on which two clusterings agree or disagree (one clustering result and the *ground truth*), such as Wallace index [56], FowlkesMallows index [57], Rand index [58], Adjusted Rand index [59], Jaccard index [60], Mirkin index [61]. In this work, we use Rand index to evaluate our proposed clustering algorithm *ADCN* and we will discuss it in detail in Section 4.

Set matching based measures match the 'best' clusters between two clustering results based on the number of shared objects, such as Clustering Error [62], the asymmetric metric proposed by Larsen et al. [63], and the metric proposed by van Dongen et al. [64]. A problem with *Set matching based measures* is that the criteria it uses completely ignore the information of the "unmatched" part of each cluster [62].

Information theoretic measures, which are based on information theory, measure the amount of mutual information shared by two clustering results via the number of objects they agree, such as Mutual Information [65], Normalize Mutual Information with different normalize methods [66, 67, 68, 69], Adjusted-for-Chance MI [52], Unnormalized distance measures [66, 62], and Normalized distance measures [68, 52]. In this work, we utilize Normalize Mutual Information from Strehl et al. [67] which we will discuss in detail in Section 4 in addition to Rand index to ensure that we use measures from different families.

All the clustering comparison measure we mentioned above are purely from a statistic perspective and treat clusterings as partitions of atoms. They compare clusterings based on the memberships of objects to different clusters. That means that an object clustered into any other clusters will be treated as equally wrong. But Zhou et al. [54], Bae et al. [53], Coen et al. [55] made an argument that miss classifying one object to different clusters will have different effects on the clustering similarity judgement. Figure 2.3 illustrates such idea. Figure 2.3 (a) shows the *ground truth* in which there are three clusters **A**, **B**, and **C**. Figure 2.3 (b) and (c) shows the clustering result of Clustering

X and **Y** in which 10 objects/points in Cluster **B'(C")** have been miss classified into Cluster **A'(A")**. Zhou et al. [54], Bae et al. [53], Coen et al. [55] argued that existing clustering comparison measures (the traditional three categories we discussed above) will yield the same similarity between the *ground truth* and Clustering **X/Y** while it is "intuitive" [53] that Clustering **X** is more similar to the *ground truth* than Clustering **Y**. That is because Cluster **B** is closer to Cluster **A** than Cluster **C**. We call this *Spatial Proximity Effect*.

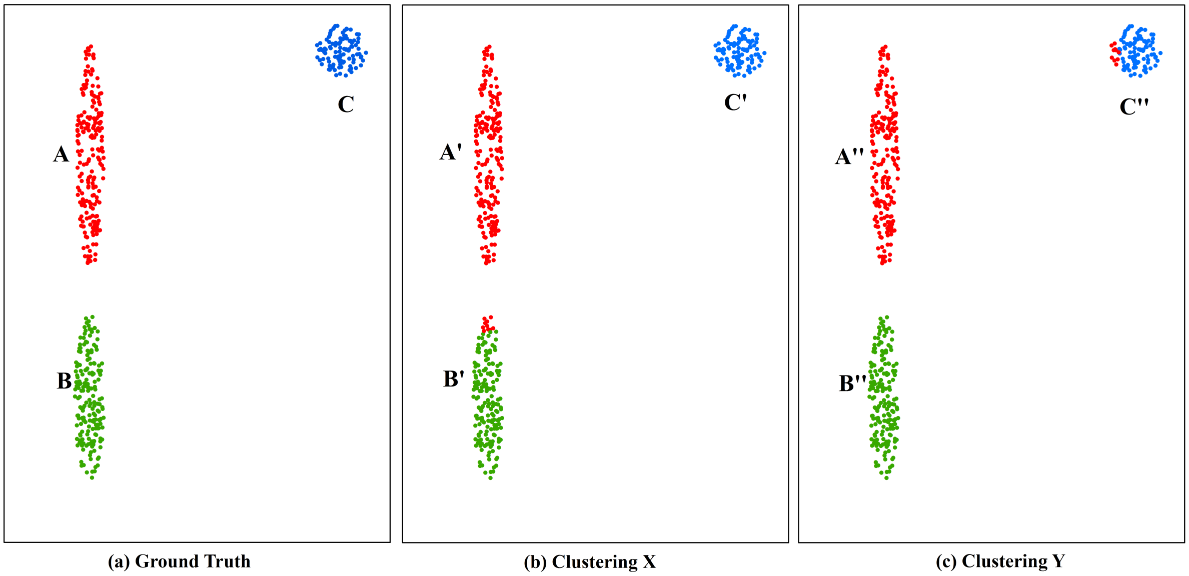

(a) Ground Truth (b) Clustering X (c) Clustering Y

Figure 2.3: An Illustration of how spatial proximity can affect the clustering comparison: (a) shows the ground truth of 3 clusters; (b) shows the result of Clustering X; (c) shows the result of Clustering Y.

Cluster similarity sensitive distance(CSS) proposed by Zhou et al. [54] applied Mallows distance function to compute clustering similarity. This makes the similarity computation become a linear programming problem in which both objects' memberships to clusters and the similarity between clusters' representatives are considered. *CSS* takes the distances between representatives of clusters into account when computing the clustering similarity. So it considers the*Spatial Proximity Effect*.

Another clustering comparison measure which considers the*Spatial Proximity Effect* is *ADCO* [53]. It segments the attribute space into high dimension grids. Each object from the dataset will occupy exactly one cell. The density profiles are computed based on this grid. And the similarity between two clusters corresponds to the similarity between distributions of the objects from each cluster over this grid. *ADCO* will match each cluster in one clustering result to one in another clustering result. This means it is more similar to *Set matching based measures.* What's more, *ADCO* requires the clusterings under consideration to have the same number of clusters which is not usually the case in real-world applications.

CDistance proposed by Coen et al. [55] also takes the *Spatial Proximity Effect* into consideration. Naive transportation distance which is also a linear programming problem has been proposed to compute the similarity distance between two weighted points sets. *CDistance* can also compare clustering result from different datasets.

It is worthy mentioning that whether spatial proximity of clusters will affect clustering similarity is still under investigation. *CSS* and *CDistance* have a much higher computation complexity compared to *Rand index* and *NMI* and are hard to implement. Hence, researchers are inclined to use the traditional clustering comparison measures which are also the choice for this work. This can also be seen from the clustering performance evaluation package of python scikit-learn library [2].

Table 2.1 lists all the clustering comparison indexes we discussed above. We compare their pros and cons from different perspectives, such as symmetry, requirements for the same number of cluster, normalized or not, the ability to compare clustering across datasets, considering spatial proximity effect or not.

---

[2] `http://scikit-learn.org/stable/modules/clustering.html#clustering-performance-evaluation`

Table 2.1: The Pros and Cons Comparison of Different Clustering Comparison Indexes

Index Class		Name	Symmetric	Require for the same number of clusters	Normalization	Compare clustering across datasets	Consider spatial proximity
pair-counting based		Wallace index [56]	No	NO	Yes	NO	NO
		Fowlkes-Mallows index [57]	Yes	NO	NO	NO	NO
		Rand index [58]	Yes	NO	Yes	NO	NO
		Adjusted Rand [59]	Yes	NO	Yes	NO	NO
		Jaccard index [60]	Yes	NO	Yes	NO	NO
		Mirkin index [61]	Yes	NO	NO	NO	NO
set-matching based		Clustering Error [62]	Yes	NO	Yes	NO	NO
		Larsen et al. [63]	NO	NO	Yes	NO	NO
		van Dongen et al. [64]	Yes	NO	NO	NO	NO
information theoretic	original	Mutual Information [65]	Yes	NO	NO	NO	NO
	Normalized MI (NMI)	NMIjoint [66]	Yes	NO	Yes	NO	NO
		NMImax [68]	Yes	NO	Yes	NO	NO
		NMIsum [68]	Yes	NO	Yes	NO	NO
		NMIsqrt [67]	Yes	NO	Yes	NO	NO
		NMImin [68]	Yes	NO	Yes	NO	NO
	Adjusted-for-Chance MI	AMImax [52]	Yes	NO	Yes	NO	NO
		AMIsum [52]	Yes	NO	Yes	NO	NO
		AMIsqrt [52]	Yes	NO	Yes	NO	NO
		AMImin [52]	Yes	NO	Yes	NO	NO
	Unnormalized distance measures	Djoint (Variation of Information) [51]	Yes	NO	NO	NO	NO
		Dmax [52]	Yes	NO	NO	NO	NO
		Dsum [52]	Yes	NO	NO	NO	NO
		Dsqrt [52]	Yes	NO	NO	NO	NO
		Dmin [52]	Yes	NO	NO	NO	NO
	Normalized distance measures	djoint (Normailized VI) [70]	Yes	NO	Yes	NO	NO
		dmax (Normailized Information Distance) [70]	Yes	NO	Yes	NO	NO
		dsum [52]	Yes	NO	Yes	NO	NO
		dsqrt [52]	Yes	NO	Yes	NO	NO
		dmin [52]	Yes	NO	Yes	NO	NO
	Adjusted-for-Chance distance measures	Admax [52]	Yes	NO	Yes	NO	NO
		Adsum [52]	Yes	NO	Yes	NO	NO
		Adsqrt [52]	Yes	NO	Yes	NO	NO
		Admin [52]	Yes	NO	Yes	NO	NO
Density profile		ADCO [53]	Yes	Yes	Yes	Yes	Yes
Mallows distance		CC [54]	Yes	NO	NO	NO	NO
		CSS [54]	Yes	NO	NO	NO	Yes
Transportation Distance		Cdistance [55]	Yes	NO	Yes	Yes	Yes

2.4 Research Question

From the discussion above, we realize that, as an important aspect of spatial data, anisotropicity , especially local anisotropicity, has not been well explored in clustering analysis. Based on this observation, we will investigate the following research question:

How to design a clustering algorithm such that:

- It is based on the same, well studied, parameters of density-based clustering techniques such as DBSCAN (namely *Eps* and *MinPts*).
- It has the same time complexity class as DBSCAN and can, therefore, operate on large datasets.
- It is better suited than DBSCAN (and density-based algorithms in general) for clustering anisotropic point patterns while remaining as good as DBSCAN for isotropic cases.

Chapter 3

Anisotropic Density-based Clustering with Noise (ADCN)

In this section we introduce the proposed **A**nisotropic **D**ensity-based **C**lustering with **N**oise (ADCN) starting with DBSCAN as foundation.

3.1 Anisotropic Perspective on Local Density

Without predefined direction information from spatial datasets, one has to compute the *local direction* for each point based on the spatial distribution of points around it. The standard deviation ellipse (SDE) [71] is a suitable method to get the major direction of a point set. In addition to the major direction (long axis), the flattening of the SDE implies how much the points are strictly distributed along the long axis. The flattening of an ellipse is calculated from its long axis a and short axis b as given by Equation 3.1:

$$f = \frac{a-b}{a} \tag{3.1}$$

Given n points, the standard deviation ellipse constructs an ellipse to represent the orientation and arrangement of these points. The center of this ellipse $O(\overline{X}, \overline{Y})$ is defined as the geometric center of these n points and is calculated by Equation 3.2:

$$\overline{X} = \frac{\sum_{i=1}^{n} x_i}{n}, \overline{Y} = \frac{\sum_{i=1}^{n} y_i}{n} \tag{3.2}$$

The coordinates (x_i, y_i) of each point are normalized to the deviation from the mean areal center point (Equation 3.3):

$$\widetilde{x_i} = x_i - \overline{X}, \widetilde{y_i} = y_i - \overline{Y}, \tag{3.3}$$

Equation 3.3 can be seen as a coordinates translation to the new origin $(\overline{X}, \overline{Y})$. If we rotate the new coordinate system counterclockwise about O by angle θ $(0 < \theta \leq 2\pi)$ and get the new coordinate system X_o-Y_o, the standard deviation along X_o axis σ_x and Y_o axis σ_y is calculated as given in Equation 3.4 and 3.5.

$$\sigma_x = \sqrt{\frac{\sum_{i=1}^{n} (\widetilde{y_i} \sin\theta + \widetilde{x_i} \cos\theta)^2}{n}} \tag{3.4}$$

$$\sigma_y = \sqrt{\frac{\sum_{i=1}^{n} (\widetilde{y_i} \cos\theta - \widetilde{x_i} \sin\theta)^2}{n}} \tag{3.5}$$

The long/short axis of SDE is along the direction who has the maximum/minimum standard deviation. Let σ_{max} and σ_{min} be the length the of semi-long axis and semi-short axis of SDE. The angle of rotation θ_m of the long/short axis is given by Equation 3.6[71].

$$\tan\theta_m = -\frac{A \pm B}{C} \tag{3.6}$$

$$A = \sum_{i=1}^{n} \widetilde{x_i}^2 - \sum_{i=1}^{n} \widetilde{y_i}^2 \tag{3.7}$$

$$C = 2\sum_{i=1}^{n} \widetilde{x_i}\widetilde{y_i} \tag{3.8}$$

$$B = \sqrt{A^2 + C^2} \tag{3.9}$$

The ± indicates two rotation angles θ_{max}, θ_{min} corresponding to long and short axis.

3.2 Anisotropic Density-Based Clusters

In order to introduce an anisotropic perspective to density-based clustering algorithms such as DBSCAN, we have to revise the definition of an *Eps*-neighborhood of a point. First, the original *Eps*-neighborhood of a point in a dataset D is defined by DBSCAN as given by Definition 1.

Definition 1 *(Eps-neighborhood of a point) The Eps-neighborhood $N_{Eps}(p_i)$ of Point p_i is defined as all the points within the scan circle centered at p_i with a radius Eps, which can be expressed as:*

$$N_{Eps}(p_i) = \{p_j(x_j, y_j) \in D | dist(p_i, p_j) \leq Eps\}$$

Such scan circle results in an isotropic perspective on clustering. However, as we discuss above, an anisotropic assumption will be more appropriate for some geographic phenomena. Intuitively, in order to introduce anisotropicity to DBSCAN, one can employ a scan ellipse instead of a circle to define the *Eps*-neighborhood of each point. Before we give a definition of the *Eps*-ellipse-neighborhood of a point, it is necessary to define a set of points around a point (Search-neighborhood of a point) which is used to derive the scan ellipse; See Definition 2.

Definition 2 *(Search-neighborhood of a point) A set of points $S(p_i)$ around Point p_i is called search-neighborhood of Point p_i and can be defined in two ways:*

1. *The Eps-neighborhood $N_{Eps}(p_i)$ of Point p_i.*
2. *The k-th nearest neighbor $KNN(p_i)$ of Point p_i. Here $k = MinPts$ and $KNN(p_i)$ does not include p_i itself.*

After determining the search-neighborhood of a point, it is possible to define the *Eps*-ellipse-neighborhood region (See Definition 3) and *Eps*-ellipse-neighborhood (See Definition 4) of each point.

Definition 3 *(Eps-ellipse-neighborhood region of a point) An ellipse ER_i is called Eps-ellipse-neighborhood region of a point p_i iff:*

1. *Ellipse ER_i is centered at Point p_i.*
2. *Ellipse ER_i is scaled from the standard deviation ellipse SDE_i computed from the Search-neighborhood $S(p_i)$ of Point p_i.*
3. $\frac{\sigma_{max}'}{\sigma_{min}'} = \frac{\sigma_{max}}{\sigma_{min}}$;

   where σ_{max}',σ_{min}' and σ_{max},σ_{min} are the length of semi-long and semi-short axis of Ellipse ER_i and Ellipse SDE_i.
4. $Area(ER_i) = \pi ab = \pi Eps^2$

According to Definition 3, the *Eps*-ellipse-neighborhood region of a point is computed based on the search-neighborhood of a point. Since there are two definitions of the search-neighborhood of a point (See Definition 2), each point should have a unique *Eps*-ellipse-neighborhood region given *Eps* (using the first definition in Definition 2) or $MinPts$ (using the second definition in Definition 2) as long as the search-neighborhood of the current point has at least two points for the computation of the standard deviation ellipse.

Definition 4 *(Eps-ellipse-neighborhood of a point) An Eps-ellipse-neighborhood* $EN_{Eps}(p_i)$ *of point* p_i *is defined as all the point inside the eillpse* ER_i*, which can be expressed as* $EN_{Eps}(p_i) = \{p_j(x_j, y_j) \in D | \frac{((y_j-y_i)\sin\theta_{max}+(x_j-x_i)\cos\theta_{max})^2}{a^2} + \frac{((y_j-y_i)\cos\theta_{max}-(x_j-x_i)\sin\theta_{max})^2}{b^2} \leq 1\}$.

There are two kinds of points in a cluster obtained from DBSCAN: *core point* and *border point*. Core points have at least $MinPts$ points in their *Eps*-neighborhood, while border points have less than $MinPts$ points in their *Eps*-neighborhood but are *density reachable* from at least one core point. Our anisotropic clustering algorithm has a similar definition of core point and border point. The notions of directly anisotropic-density-reachable and core point are illustrated bellow; see Definition 5.

Definition 5 *(Directly anisotropic-density-reachable) A point* p_j *is directly anisotropic density reachable from point* p_i *wrt. Eps and* $MinPts$ *iff:*

1. $p_j \in EN_{Eps}(p_i)$.

2. $|EN_{Eps}(p_i)| \geq MinPts$. *(Core point condition)*

If point p is directly anisotropic reachable from point q, then point q must be a core point which has no less than $MinPts$ points in its *Eps*-ellipse-neighborhood. Similar to the notion of density-reachable in DBSCAN, the notion of anisotropic-density-reachable is given in Definition 6.

Definition 6 *(Anisotropic-density-reachable) A point* p *is anisotropic density reachable from point* q *wrt. Eps and* $MinPts$ *if there exists a chain of points* p_1, p_2, ..., p_n, *(*$p_1 = q$, *and* $p_n = p$*) such that point* p_{i+1} *is directly anisotropic density reachable from* p_i.

Although anisotropic density reachability is not a symmetric relation, if such a directly anisotropic density reachable chain exits, then except for point p_n, the other $n-1$ points are all core points. If Point p_n is also a core point, then symmetrically point p_1 is also density reachable from p_n. That means that if two points p, q are anisotropic density reachable from each other, then both of them are core points and belong to the same cluster.

Equipped with the above definitions, we are able to define our anisotropic density-based notion of clustering. DBSCAN includes both core points and border points into its clusters. In our clustering algorithm, only core points will be treated as cluster points. Border points will be excluded from clusters and treated as noise points, because otherwise many noise points will be included into clusters according to experimental results. In short, a cluster (See definition 7) is defined as a subset of points from the whole points dataset in which each two points are anisotropic density reachable from another. Noise points (See Definition 8) are defined as the subset of points from the entire points dataset for which each point has less than $MinPts$ points in its *Eps*-ellipse-neighborhood.

Definition 7 *(Cluster) Let* D *be a points dataset. A cluster* C *is a no-empty subset of* D *wrt. Eps and* $MinPts$*, iff:*

1. $\forall p \in C$, $EN_{Eps}(p) \geq MinPts$.

2. $\forall p, q \in C$, p, q *are anisotropic density reachable from each other wrt. Eps and* $MinPts$.

A cluster C has two attribute:

$\forall p \in C$ and $\forall q \in D$, if p is anisotropic density reachable from q wrt. Eps and $MinPts$, then

1. $q \in C$.
2. There must be a directly anisotropic density reachable points chain $C(q,p)$: p_1, p_2, ..., p_n, ($p_1 = q$, and $p_n = p$), such that p_{i+1} is directly anisotropic density reachable from p_i. Then $\forall p_i \in C(q,p)$, $p_i \in C$.

Definition 8 *(Noise) Let D be a points dataset. A point p is a noise point wrt. Eps and $MinPts$, if $p \in D$ and $EN_{Eps}(p) < MinPts$.*

Let C_1, C_2, ..., C_k be the clusters of the points dataset D wrt. Eps and $MinPts$. From Definition 8, if $p \in D$, and $EN_{Eps}(p) < MinPts$, then $\forall C_i \in \{C_1, C_2, ..., C_k\}$, $p \notin C_i$.

According to Definition 2, and in contrast to a simple scan circle, there are at least two ways to define a search neighborhood of the center point p_i. Thus, ADCN can be divided into a ADCN-Eps variant that uses *Eps*-neighborhood $N_{Eps}(p_i)$ as the search neighborhood and ADCN-KNN that uses k-th nearest neighbors $KNN(p_i)$ as the search neighborhood. Figures 3.1 and 3.2 illustrates the related definitions for ADCN-Eps and ADCN-KNN. The red points in both figures represent current center points. The blue points indicate the two different search neighborhoods of the corresponding center points according to Definition 2. Note that for ADCN-Eps, the center point is also part of its search neighborhood which is not true for ADCN-KNN. The green ellipses and green crosses stand for the standard deviation ellipses constructed from the corresponding search neighborhood and their center points. The red ellipses are *Eps*-ellipse-neighborhood regions while the dash line circles indicate a DBSCAN-like scan circle. As can be seen, ADCN-

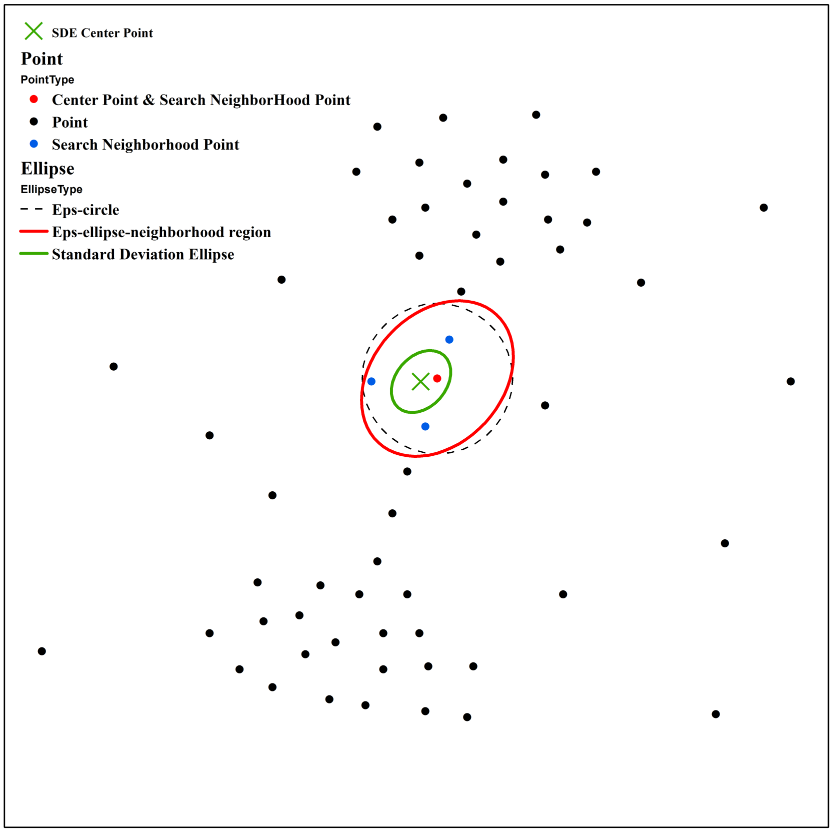
SDE Center Point
Point
PointType
Center Point & Search NeighborHood Point
Point
Search Neighborhood Point
Ellipse
EllipseType
Eps-circle
Eps-ellipse-neighborhood region
Standard Deviation Ellipse

Figure 3.1: Illustration for ADCN-Eps

KNN will exclude the point to the left of the linear *bridge*-pattern while DBSCAN would include it.

3.3 ADCN Algorithms

From the definitions provided above it follows that our *anisotropic density-based clustering with noise* algorithm takes the same parameters ($MinPts$ and *Eps*) as DBSCAN and that they have to be decided before clustering. This is for good reasons, as the proper selection of DBSCAN parameters has been well studied and ADCN can easily replace DBSCAN without any changes to established workflows.

As shown in Algorithm 1, ADCN starts with an arbitrary point p_i in a points dataset

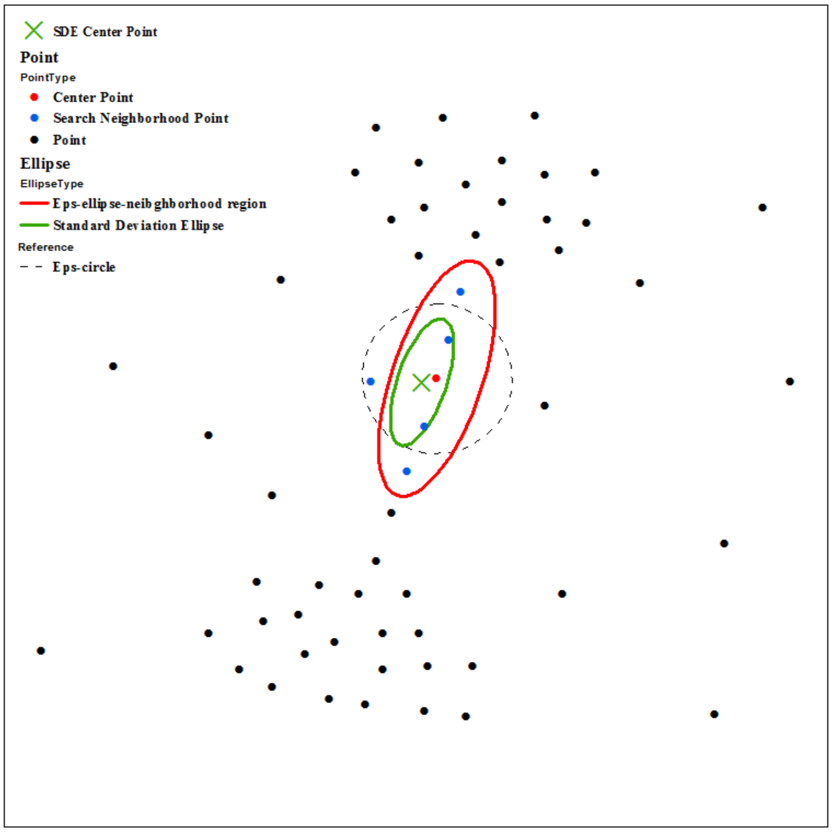

Figure 3.2: Illustration for ADCN-KNN

D and discovers all the *core* points which are anisotropic density reachable from point p_i. According to Definition 2, there are two ways to get the search neighborhood of point p_i which will result in different *Eps*-ellipse-neighborhood $EN_{Eps}(p_j)$ based on the derived *Eps*-ellipse-neighborhood-region in Algorithm 2. Hence, ADCN can be implemented by two algorithms (ADCN-Eps, ADCN-KNN). Algorithm 2 needs to take care of situations when all points of the Search-neighborhood $S(p_i)$ of Point p_i are *strictly* on the same line. In this case, the short axis of *Eps*-ellipse-neighborhood region ER_i becomes *zero* and its long axis become *Infinity*. This means $EN_{Eps}(p_i)$ is diminished to a straight line. The process of constructing *Eps*-ellipse-neighborhood $EN_{Eps}(p_i)$ of Point p_i becomes a point-on-line query.

Algorithm 1: ADCN(D, $MinPts$, Eps)

```
Input  : A set of n points $D(X, Y)$ ; $MinPts$; $Eps$;
Output: Clusters with different labels $C_i[]$; A set of noise points $Noi[]$
foreach point $p_i(x_i, y_i)$ in the set of points $D(X, Y)$ do
    Mark $p_i$ as $Visited$;
    //Get $Eps$-ellipse-neighborhood $EN_{Eps}(p_i)$ of $p_i$
    ellipseRegionQuery($p_i$, $D$, $MinPts$, $Eps$);
    if $|EN_{Eps}(p_i)| < MinPts$ then
        Add $p_i$ to the noise set $Noi[]$;
    else
        Create a new Cluster $C_i[]$;
        Add $p_i$ to $C_i[]$;
        foreach point $p_j(x_j, y_j)$ in $EN_{Eps}(p_i)$ do
            if $p_j$ is not visited then
                Mark $p_j$ as visited;
                //Get $Eps$-ellipse-neighborhood $EN_{Eps}(p_j)$ of Point $p_j$
                ellipseRegionQuery($p_j$, $D$, $MinPts$, $Eps$);
                if $|EN_{Eps}(p_j)| \geq MinPts$ then
                    Let $EN_{Eps}(p_i)$ as the merged set of $EN_{Eps}(p_i)$ and $EN_{Eps}(p_j)$;
                    Add $p_j$ to current cluster $C_i[]$;
                else
                    Add $p_j$ to the noise set $Noi[]$;
                end
            end
        end
    end
end
```

According to Algorithm 3, ADCN-Eps uses the Eps-neighborhood $N_{Eps}(p_i)$ of point p_i as the search neighborhood which will be used later to construct the standard deviation ellipse. In contrast, ADCN-KNN (Algorithm 4) uses a k-th nearest neighborhood of point p_i as the search neighborhood. Here point p_i will not be included in its k-th nearest neighborhood. As can be seen, the run times of ADCN-Eps and ADCN-KNN are heavily dominated by the search-neighborhood query which is executed on each point. Hence, the time complexities of ADCN, DBSCAN, and OPTICS are O(n^2) without a spatial index and O(n log n) otherwise.

Algorithm 2: ellipseRegionQuery(p_i, D, $MinPts$, Eps)

```
Input  : $p_i$, $D$, $MinPts$, $Eps$
Output: $Eps$-ellipse-neighborhood $EN_{Eps}(p_i)$ of Point $p_i$
//Get the Search-neighborhood $S(p_i)$ of Point $p_i$. ADCN-Eps and ADCN-KNN use different functions.
ADCN-Eps: searchNeighborhoodEps($p_i$, $D$, $Eps$); ADCN-KNN: searchNeighborhoodKNN($p_i$, $D$, $MinPts$);
Compute the standard deviation ellipse $SDE_i$ base on the Search-neighborhood $S(p_i)$ of Point $p_i$;
Scale Ellipse $SDE_i$ to get the $Eps$-ellipse-neighborhood region $ER_i$ of Point $p_i$ to make sure $Area(ER_i) = \pi \times Eps^2$;
if The length of short axis of $ER_i == 0$ then
    // the $Eps$-ellipse-neighborhood region $ER_i$ of Point $p_i$ is diminished to a straight line. Get $Eps$-ellipse-neighborhood $EN_{Eps}(p_i)$ of Point $p_i$ by finding all points on this straight line $ER_i$;
else
    // the $Eps$-ellipse-neighborhood region $ER_i$ of Point $p_i$ is an ellipse. Get $Eps$-ellipse-neighborhood $EN_{Eps}(p_i)$ of Point $p_i$ by finding all the points inside Ellipse $ER_i$;
end
return $EN_{Eps}(p_i)$;
```

Algorithm 3: searchNeighborhoodEps(p_i, D, Eps)

```
Input  : $p_i$, $D$, $Eps$
Output: the Search-neighborhood $S(p_i)$ of Point $p_i$
// This function is used in ADCN-Eps // Get all the points whose distance from Point $p_i$ is less than $Eps$
foreach point $p_j(x_j, x_j)$ in the set of points $D(X, Y)$ do
    if $\sqrt{(x_i - x_j)^2 + (y_i - y_j)^2} \leq Eps$ then
        Add Point $p_j$ to $S(p_i)$;
end
return $S(p_i)$;
```

Algorithm 4: searchNeighborhoodKNN(p_i,D,$MinPts$)

```
Input   : $p_i$; $D$; $MinPts$
Output: the Search-neighborhood $S(p_i)$ of Point $p_i$
// This function is used in ADCN-KNN // Get the Kth nearest neighbor of Point
  $p_i$ excluding $p_i$ itself
KNNArray = new Array($MinPts$);
distanceArray = new Array($|D|$);
KNNLabelArray = new Array($|D|$);
foreach point $p_j(x_j, y_j)$ in the set of points $D(X, Y)$ do
    KNNLabelArray[j] = 0;
    distanceArray[j] = $\sqrt{(x_i - x_j)^2 + (y_i - y_j)^2}$;
    if $j == i$ then
        KNNLabelArray[j] = 1;
end
foreach $k$ in 0:($MinPts - 1$) do
    minDist = Infinity;
    minDistID = 0;
    foreach $j$ in 0:$|D|$ do
        if KNNLabelArray[j] != 1 then
            if minDist > distanceArray[j] then
                minDist = distanceArray[j];
                minDistID = j;
    end
    KNNLabelArray[minDistID] = 1;
    KNNArray[k] = minDistID;
    Add the point with minDistID as ID to $S(p_i)$;
end
return $S(p_i)$;
```

Chapter 4

Experiments and Performance Evaluation

In this section, we will evaluate the performance of ADCN from two perspectives: clustering quality and clustering efficiency. In contrast to the scan circle of DBSCAN, there are at least two ways to determine an anisotropic neighborhood. This leads to two realizations of ADCN, namely ADCN-KNN and ADCN-Eps. We will evaluate their performance using DBSCAN and OPTICS as baselines. We selected OPTICS as an additional baseline as it is commonly used to address some of DBSCAN's shortcomings with respect to varying densities.

According to the research contributions outlined in Section 1, we intend to establish: **(1)** that at least one of the ADCN variants performs as good as DBSCAN (and OPTICS) for cases that do not explicitly benefit from an anisotropic perspective; **(2)** that the aforementioned variant performs better than the baselines for cases that *do* benefit from an anisotropic perspective; and finally **(3)** that the test cases include point patterns typically used to test density-based clustering algorithms as well as *real-world* cases that highlight the need for developing ADCN in the first place. In addition, we will show runtime results for all four algorithms.

4.1 Experiment Designs

We have designed several spatial point patterns as test cases for our experiments. More specifically, we generated 20 test cases with 3 different noise settings for each of them. These consist of 12 synthetic and 8 real-world use cases which results in a total of **60** case studies. Note that our test cases do not only contain linear features such as road networks but also cases that are typically used to evaluate algorithms such as DBSCAN, e.g., clusters of ellipsoid and rectangular shapes.

In order to simulate a "ground truth" for the synthetic cases, we created polygons to indicate different clusters and randomly generated points within these polygons and outside of them. We took a similar approach for the eight real-world cases. The only difference is that the polygons for real world cases have been generated from buffer zones with a 3-meter radius of the real-world features, e.g., existing road networks. This allows us to simulate patterns that typically occur in geo-tagged social media data.

Although we use this approach to simulate the corresponding spatial point process, the distinction between clustered points and noise points in the resulting spatial point patterns may not be so obvious even from a human's perspective. To avoid cases in which it is unreasonable to expect algorithms and humans to differentiate between noise and pattern, we introduced a clipping buffer of 0m, 5m, and 10m. For comparison, the typical position accuracy of GPS sensors on smartphones and GPS collars for wildlife tracking is about 3-15 meters [72](and can decline rapidly in urban canyons).

The generated spatial point patterns of 12 synthetic and 8 real-world use cases with 0m buffer distance are shown in the first column of Figure 4.2 and Figure 4.3. Note that in all test cases, points generated from different polygons are pre-labeled with different cluster IDs which are indicated by different colors in the first column of Figure 4.2 and Figure 4.3. Points generated outside polygons are pre-labeled as *noise* which are shown in *black*. These generated spatial point patterns serve as *ground truth* which are used in our clustering quality evaluation experiments.

In order to demonstrate the strength of ADCN, we need to compare the performance of ADCN with that of DBSCAN and OPTICS from two perspectives: clustering quality and clustering efficiency. The experiment designs are as follow:

- As for clustering quality evaluation, we use several clustering quality indices to quantify how good the clustering results are. In this work, we use Normalized Mutual Information (NMI) and the Rand Index. We will explain these two indices in detail in Section 4.3. We stepwise tested every possible parameter combinations of Eps, $MinPts$ computationally on each test case. For each clustering algorithm, we select the parameter combination which has the highest NMI or Rand index. By comparing the maximum of NMI and Rand index across different clustering algorithms in each test case, we can find out the best clustering technique.
- As for clustering efficiency evaluation, we generate spatial point patterns with different numbers of points by using the polygons of each test case mentioned earlier. For each clustering algorithm and each number of points setting, we computed the average runtime. By constructing a runtime curve of each clustering algorithm, we are able to compare their runtime efficiency.

4.2 Test Environment

In order to compare the performance of ADCN with that of DBSCAN and OPTICS, we developed a JavaScript test environment to generate patterns and compare the results.

It allows us to generate use cases in a Web browser, such as Firefox or Chrome, or load them from a GIS, change noise settings, determine DBSCAN's Eps via a KNN distance plot, perform different evaluations, compute runtimes, index the data via an R-tree, and save and load the data. Consequently, what matters is the *runtime behavior*, not the exact performance (for which JavaScript would not be a suitable choice). All cases have been performed on a *cold* setting, i.e., without any caching using an Intel i5-5300U CPU with 8 GB RAM on an Ubuntu 16.04 system. This Javascript test environment as well as all the test cases can be downloaded from here[1].

Figure 4.1 shows a snapshot of this test environment. The system has two main panels. The map panel on the left side is an interactive canvas in which the user can click and create data points. The tool bar on the right side is composed of input boxes, selection boxes, and buttons which are divided into different groups. Each group is used for a specific purpose, which will be discussed as below.

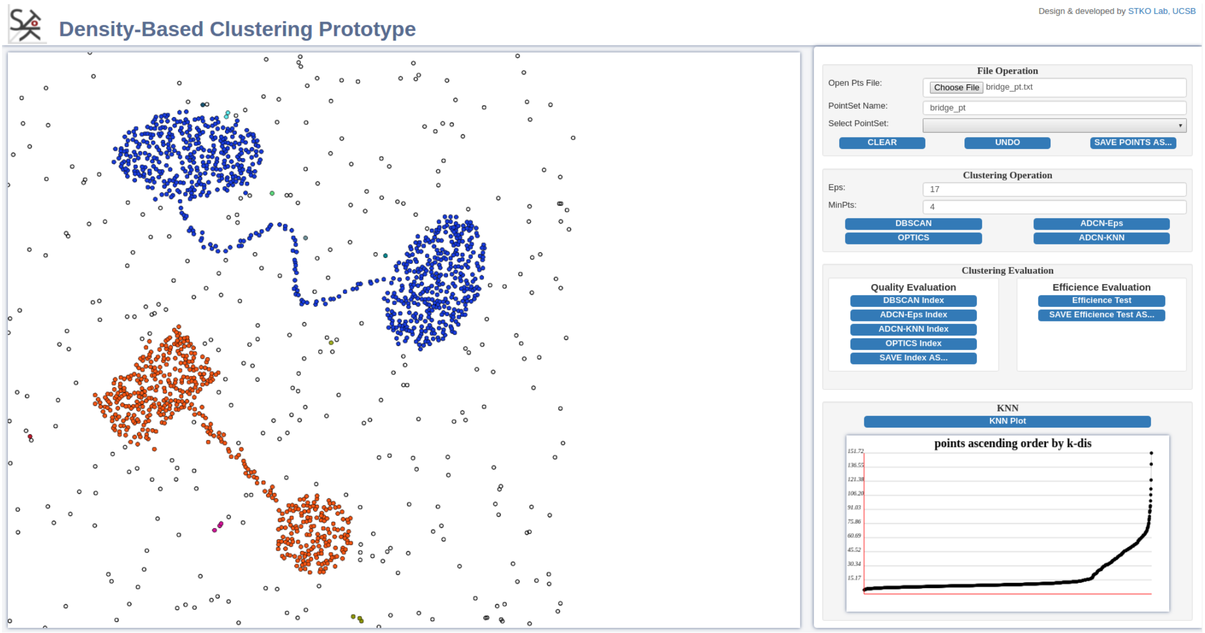

Open Pts File: bridge_pt.txt

PointSet Name: bridge_pt

Eps: 17

MinPts: 4

Figure 4.1: The Density-Based Clustering Test Environment

---

[1] `http://stko.geog.ucsb.edu/adcn/`

The “File Operation” tool group is used for point dataset manipulation. For simplicity, our environment defines a simple format for point datasets. Conceptually, a point dataset is a table containing the coordinates of points, their ground truth memberships, and the memberships produced during the experiments. The ground truth and experimental memberships are then compared to evaluate the cluster algorithms. The “Open Pts File” box is used for loading point datasets produced by other GIS. The data points can also be abstract points which represent objects, such as documents [7], in a feature space. The prototype takes the coordinates of points and maps out these points after rescaling their coordinates based on the size of the map panel. During the clustering process it uses Euclidean distance as the distance measure. The “PointSet Name” input box lets the user name the current point dataset displayed on the map panel. The “Select PointSet” selection box lists all the point datasets loaded into the system.

The “Clustering Operation” tool group is used to operate clustering tasks. The “Eps” and “MinPts” input boxes let users enter the clustering parameters for all clustering algorithms. The “DBSCAN”, “OPTICS”, “ADCN-Eps”, “ADCN-KNN” buttons are for running the algorithms. A user can click one of them to run the corresponding clustering algorithm on current point dataset based on the parameters (s)he entered earlier. As for the implementation of DBSCAN and OPTICS, we used a JavaScript clustering library from GitHub [2]. This library has basic implementations of DBSCAN, OPTICS, K-MEANS, and some other clustering algorithms without any spatial indexes. Our ADCN-KNN and ADCN-Eps algorithms were implemented using the same data structures as used in the library. Such an implementation ensures that the evaluation result will reflect the differences of the algorithms rather than be affected by the specific data structures used in the implementations. Finally, we implemented an R-tree spatial index to accelerate the neighborhood search. We have used the R-tree JavaScript library

---

[2] `https://github.com/uhho/density-clustering`

from GitHub [3].

The “Clustering Evaluation” tool group is composed of “Quality Evaluation” and “Efficiency Evaluation” subgroups. As for the clustering quality evaluation, we implemented two metrics, Normalized mutual Information (NMI) and Rand Index, to quantify the goodness of the clustering results. The first four buttons in this subgroup will run the corresponding clustering algorithm on the current dataset based on all possible parameter combinations. They will compute two clustering evaluation indexes for each clustering result. The “SAVE Index As...” button will save these results to a text file.

Efficiency evaluation is another important part for comparing clustering algorithms. Density-based clustering algorithms are widely applied on large-scale data points. Therefore it is important to demonstrate the scalability of ADCN. The “Efficiency Evaluation” button will run these four clustering algorithms on datasets with different sizes. The “SAVE Efficiency Test As...” button can be further used to save the result into a text file.

Finally, the “KNN” tool group is used to draw the k_{th} *nearest neighbor plot* (KNN plot) of the current dataset based on the *MinPts* parameter specified by the user. For each point, the KNN plot obtains the distance between the current point and its k_{th} nearest point (here K is *MinPts*). Then it ranks these k_{th} nearest distance of each point in an ascending order. The KNN plot can be used for estimating the appropriate *Eps* for the current point dataset given *MinPts*. More details this estimation can be found in the original DBSCAN paper [8].

Note that we provide the test environment to make our results reproducible and to offer a reusable implementation of ADCN, without implying that JavaScript would be the language of choice for future, large-scale applications of ADCN.

---

[3] `https://github.com/imbcmdth/RTree`

4.3 Evaluation of Clustering Quality

We use two clustering quality indices - the normalized mutual information (NMI) and the Rand Index - to measure the quality of clustering results of all algorithms. NMI originates from information theory and has been revised as an objective function for clustering ensembles [67]. NMI evaluates the accumulated mutual information shared by the clusters from different clustering algorithms. Let n be the number of points in a point datasets D. $X = (X_1, X_2, ..., X_r)$ and $Y = (Y_1, Y_2, ..., Y_s)$ are two clustering results from the same or different clustering algorithms. Note that noise points will be treated as their own cluster. Let $n_h^{(x)}$ be the number of points in cluster X_h and $n_l^{(y)}$ the number of points in cluster Y_l. Let $n_{h,l}^{(x,y)}$ be the number of points in the intersect of cluster X_h and Y_l. Then the normalized mutual information $\Phi^{(NMI)}(X, Y)$ is defined in Equation 4.1 as the similarity between two clustering results X and Y:

$$\Phi^{(NMI)}(X,Y) = \frac{\sum_{h=1}^{r}\sum_{l=1}^{s} n_{h,l}^{(x,y)} \log \frac{n \cdot n_{h,l}^{(x,y)}}{n_h^{(x)} \cdot n_l^{(y)}}}{\sqrt{(\sum_{h=1}^{r} n_h^{(x)} \log \frac{n_h^{(x)}}{n})(\sum_{l=1}^{s} n_l^{(y)} \log \frac{n_l^{(y)}}{n})}} \tag{4.1}$$

Rand Index [58] is another objective function for clustering ensembles from a different perspective. It evaluates to which degree two clustering algorithms share the same relationships between points. Let a be the number of pairs of points in D that are in the same clusters in X and in the same cluster in Y. b is the number of pairs of points in D that are in different clusters in X and Y. c is the number of pairs of points in D that are in the same clusters in X and in different cluster in Y. Finally, d is the number of pairs of points in D that are in different clusters in X and in the same cluster in Y. The Rand Index $\Phi^{(Rand)}(X, Y)$ is then defined as given by Equation 4.2:

$$\Phi^{(Rand)}(X, Y) = \frac{a + b}{a + b + c + d} \tag{4.2}$$

For both NMI and Rand index, larger values indicate higher similarity between two clustering results. If a ground truth is available, both NMI and Rand can be used to compute the similarity between the result of an algorithms and the corresponding ground truth. This is called the *extrinsic method* [21].

We use the aforementioned 20 test cases to evaluate the clustering quality of DBSCAN, ADCN-Eps, ADCN-KNN, and OPTICS. All of these four algorithms take the same parameters (Eps, $MinPts$). As there are no established methods to determine the best overall parameter combination (we use KNN distance plots to estimate Eps) with respect to NMI and Rand Index, we stepwise tested every possible parameter combinations of Eps, $MinPts$ computationally. An interactive 3D visualization of the NMI and Rand index results with changing Eps and $MinPts$ for the *spiral* case with 0m buffer distance can be accessed online [4]. Table 4.1 shows the maximum NMI and Rand Index results for the four algorithms over all test cases. Note that for each case, the best parameter combination with the maximum NMI does not necessarily yields the maximum Rand Index. However, among all of these 60 cases, there are 39, 35, 27, 39 cases for DBSCAN, ADCN-Eps, ADCN-KNN, OPTICS in which the best parameter combination for the maximum NMI is also the maximum Rand Index. For those cases where parameter combinations of maximum NMI and maximum Rand do not match, their parameters tend to be close to each other because NMI and Rand values are changing continuously while Eps and $MinPts$ increase. This indicates that NMI and Rand Index have a medium to high similarity in terms of measuring the clustering quality.

---

[4] `http://stko.geog.ucsb.edu/adcn/`

As for the 60 test cases, ADCN-KNN has a higher maximum NMI/Rand Index than DBSCAN in **55** cases and has a higher maximum NMI/Rand Index than OPTICS in **55** cases; see also Figures 4.4 and 4.5. Even more, ADCN-KNN has a higher maximum NMI/Rand Index than ADCN-Eps in **31** cases; see Table 4.2. This indicates that ADCN-KNN gives the best clustering results among the tested algorithms. Our test cases do not only contain linear features but also cases that are typically used to evaluate algorithms such as DBSCAN, e.g., clusters of ellipsoid and rectangular shapes. In fact, these are the only cases were DBSCAN slightly out-competes ADCN-KNN, i.e., the maximum NMI/Rand Index of ADCN-KNN and DBSCAN are comparable. Summing up, ADCN-KNN performs better than all other algorithms when dealing with anisotropic cases and equally well as DBSCAN for isotropic cases. In the following paragraphs, we will use ADCN-KNN and ADCN interchangeably.

Figure 4.2 and 4.3 show the point patterns as well as the best clustering results of all algorithms for the twelve synthesis cases and eight real-world cases without buffering, i.e., with the 0m buffer distance. By comparing best clustering results of these four algorithms, we can find some interesting patterns: 1) *Connecting clusters along local directions*: ADCN has a better ability to detect the local direction of spatial point patterns and connect the clusters along this direction; 2) *Noise filtering*: ADCN does better in filtering out noise points. A good example of *connecting clusters along local directions* is the *ellipseWidth* case in Figure 4.2. As for the thinnest cluster in the bottom, the other 3 algorithms except ADCN-KNN extract multiple clusters from these points while ADCN-KNN is able to "connect" these clusters to a single one. Many cases show the *noise filtering* advantage of ADCN. For example, the*bridge* case, the *multiBridge* case in Figure 4.2, and the*Brooklyn Bridge* case in Figure 4.3, reveal that ADCN is better at detecting and filtering out noise points along bridge-like features.

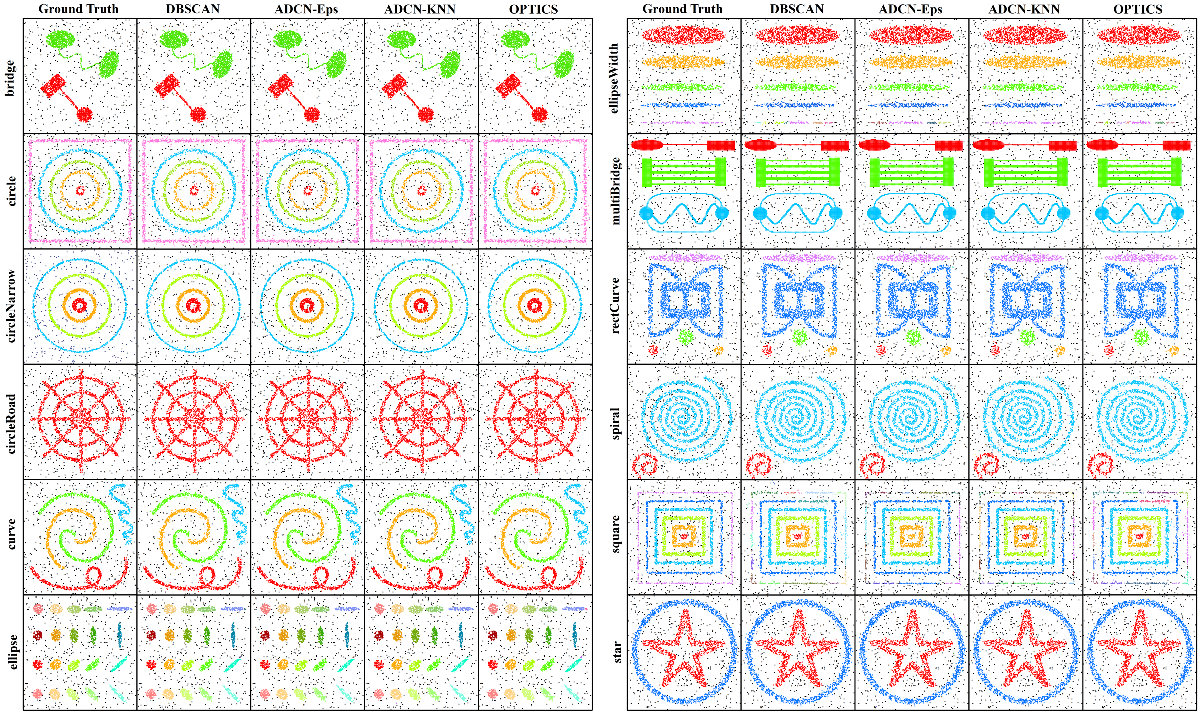

(a) (b)

Figure 4.2: Ground truth and best clustering result comparison for 12 synthesis cases.

4.4 Evaluation of Clustering Efficiency

This section discusses runtime differences of the four tested algorithms. Without a spatial index, the time complexity of all algorithms is O(n^2). *Eps*-neighborhood queries consume the major part of the run time of density-based clustering algorithms [9], and, therefore, also of ADCN-KNN and ADCN-Eps in terms of *Eps*-ellipse-neighborhood queries. Hence, we implemented an R-tree to accelerate the neighborhood queries for all algorithms. This changes their time complexity to O(n log n).

In order to enable a comprehensible comparison of the run times of all algorithms on different sizes of point datasets, we performed a batch of performance tests. The polygons from the 20 cases shown above have been used to generated point datasets of different sizes ranging from 500 to 10000 in 500 step intervals. The ratio of noise points to cluster points is set to 0.25. Eps, $MinPts$ are set to 15, 5 for all of these experiments. The average run times for the same size of point datasets is depicted in Figure 4.6.

Unsurprisingly, the runtime of all algorithms increases as the number of points increases. The runtime of ADCN-KNN is larger than that of DBSCAN and similar that of OPTICS. As the size of the point dataset increases, the ratio of the runtimes of ADCN-KNN to DBSCAN decrease from 2.80 to 1.29. The original OPTICS paper states a 1.6 runtime factor compared to DBSCAN. The used OPTICS library failed on datasets exceeding 5500 points. We also fit the runtime data to the $xlog(x)$ function. Figure 4.6 shows the fitted curves and functions of each clustering algorithm. We can see that all R^2 of these functions are larger than 0.95 which means that the $xlog(x)$ function well captures the trends of the real runtime data of these clustering algorithms. For ADCN, our implementation tests for point-in-circle for the radius of the major axis before computing point-in-ellipse to significantly reduce the runtime. Further implementation optimizations are possible but out of scope of this paper.

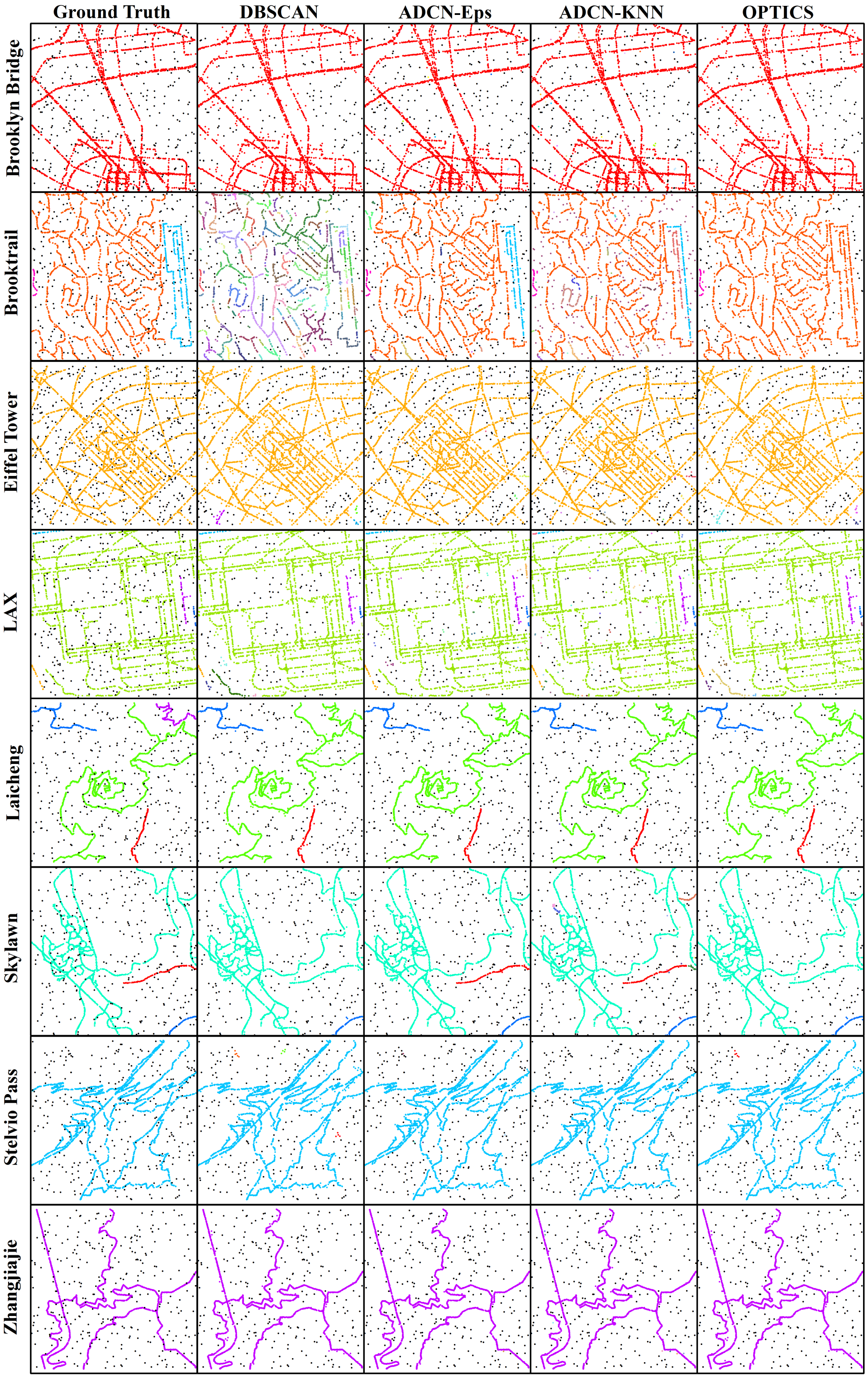

Figure 4.3: Ground truth and best clustering result comparison for eight real-world cases.

Table 4.1: Clustering quality comparisons

		NMI				Rand			
Case	Buffer	DBSCAN	ADCN-Eps	ADCN-KNN	OPTICS	DBSCAN	ADCN-Eps	ADCN-KNN	OPTICS
bridge	0m	0.937	**0.957**	**0.957**	0.937	0.985	0.991	**0.992**	0.985
	5m	0.948	0.966	**0.967**	0.949	0.989	0.993	**0.994**	0.989
	10m	0.938	**0.973**	0.968	0.944	0.988	**0.995**	**0.995**	0.989
circle	0m	0.864	0.865	**0.912**	0.864	0.955	0.964	**0.978**	0.955
	5m	0.859	0.897	**0.916**	0.859	0.955	0.974	**0.978**	0.955
	10m	0.864	0.911	**0.923**	0.864	0.960	0.979	**0.982**	0.960
circleNarrow	0m	0.914	0.951	**0.958**	0.914	0.974	0.988	**0.991**	0.974
	5m	0.939	0.946	**0.965**	0.939	0.983	0.987	**0.993**	0.983
	10m	0.923	**0.962**	**0.962**	0.923	0.976	0.991	**0.992**	0.976
circleRoad	0m	0.689	0.704	**0.725**	0.689	0.934	0.945	**0.952**	0.934
	5m	0.737	0.758	**0.779**	0.737	0.950	**0.963**	0.962	0.951
	10m	0.730	0.778	**0.821**	0.730	0.946	0.963	**0.971**	0.946
curve	0m	0.918	0.946	**0.955**	0.918	0.978	0.989	**0.991**	0.978
	5m	0.924	0.947	**0.956**	0.924	0.980	0.990	**0.992**	0.980
	10m	0.916	0.943	**0.947**	0.916	0.978	0.988	**0.989**	0.978
ellipse	0m	0.978	**0.982**	0.976	0.978	0.996	**0.997**	0.995	0.996
	5m	0.979	**0.982**	0.980	0.979	0.996	**0.997**	0.996	0.996
	10m	0.975	**0.980**	0.978	0.974	0.996	**0.997**	0.996	0.996
ellipseWidth	0m	0.917	**0.935**	**0.935**	0.917	0.985	**0.989**	0.988	0.985
	5m	0.919	0.933	**0.939**	0.919	0.988	**0.989**	**0.989**	0.988
	10m	0.931	0.938	**0.941**	0.931	0.990	**0.991**	**0.991**	0.989
multiBridge	0m	0.935	0.790	**0.957**	0.938	0.983	0.935	**0.992**	0.984
	5m	0.958	0.883	**0.977**	0.958	0.992	0.968	**0.996**	0.992
	10m	0.964	0.830	**0.985**	0.964	0.994	0.947	**0.998**	0.994
rectCurve	0m	0.886	0.893	**0.907**	0.886	0.963	0.969	**0.973**	0.963
	5m	0.909	0.910	0.908	**0.915**	0.974	**0.977**	0.974	0.974
	10m	0.921	**0.923**	0.911	0.922	0.975	**0.977**	**0.977**	0.975
spiral	0m	0.740	0.756	**0.774**	0.740	0.913	0.930	**0.938**	0.913
	5m	0.776	**0.812**	0.809	0.776	0.927	0.946	**0.948**	0.927
	10m	0.745	0.788	**0.795**	0.745	0.918	0.950	**0.952**	0.918
square	0m	0.745	0.751	**0.794**	0.745	0.934	0.920	**0.944**	0.934
	5m	0.751	0.778	**0.830**	0.752	0.932	0.928	**0.959**	0.932
	10m	0.744	0.716	**0.801**	0.743	0.935	0.893	**0.944**	0.935
star	0m	0.887	0.901	**0.914**	0.887	0.968	0.977	**0.980**	0.968
	5m	0.903	0.899	**0.916**	0.900	0.974	0.977	**0.982**	0.974
	10m	0.902	0.778	**0.909**	0.902	0.974	0.924	**0.981**	0.974
Brooklyn Bridge	0m	0.378	**0.542**	0.490	0.378	0.888	**0.930**	0.925	0.888
	5m	0.442	**0.604**	0.579	0.440	0.900	**0.943**	0.941	0.900
	10m	0.504	**0.639**	0.581	0.507	0.915	**0.950**	0.944	0.915
Brooktrail	0m	**0.441**	0.431	0.421	0.440	0.742	**0.765**	0.756	0.742
	5m	0.476	**0.512**	0.489	0.475	0.750	**0.825**	0.800	0.750
	10m	0.387	**0.555**	0.498	0.387	0.712	**0.852**	0.799	0.711
Eiffel Tower	0m	0.397	0.481	**0.492**	0.397	0.851	0.882	**0.898**	0.851
	5m	0.459	0.566	**0.571**	0.459	0.868	0.906	**0.921**	0.868
	10m	0.411	**0.553**	**0.553**	0.411	0.861	0.907	**0.923**	0.861
LAX	0m	0.557	**0.607**	0.593	0.557	0.867	0.898	**0.905**	0.867
	5m	0.591	**0.667**	0.584	0.591	0.883	**0.921**	0.903	0.883
	10m	0.485	0.590	**0.637**	0.479	0.857	0.903	**0.925**	0.857
Laicheng	0m	0.768	**0.807**	0.804	0.768	0.857	**0.874**	**0.874**	0.857
	5m	0.761	**0.815**	0.808	0.761	0.856	0.878	**0.905**	0.856
	10m	0.773	**0.823**	0.809	0.773	0.861	0.880	**0.911**	0.861
Skylawn	0m	0.618	**0.822**	0.733	0.618	0.871	**0.956**	0.927	0.871
	5m	0.642	0.690	**0.807**	0.642	0.877	0.899	**0.955**	0.877
	10m	0.729	0.703	**0.822**	0.729	0.927	0.905	**0.957**	0.927
Stelvio Pass	0m	0.640	0.715	**0.717**	0.656	0.945	0.962	**0.963**	0.946
	5m	0.739	**0.791**	0.768	0.739	0.962	0.974	**0.975**	0.962
	10m	0.686	**0.798**	0.766	0.686	0.953	0.975	**0.978**	0.953
Zhangjiajie	0m	0.760	**0.832**	0.799	0.760	0.964	**0.978**	0.976	0.964
	5m	0.772	**0.868**	0.839	0.772	0.967	**0.987**	0.982	0.967
	10m	0.835	**0.911**	0.873	0.835	0.978	**0.991**	0.990	0.978

Table 4.2: The number of cases with maximum NMI/Rand for each clustering algorithm

# of cases	Max NMI	Max Rand
DBSCAN	1	0
ADCN-Eps	25	19
ADCN-KNN	33	41
OPTICS	1	0

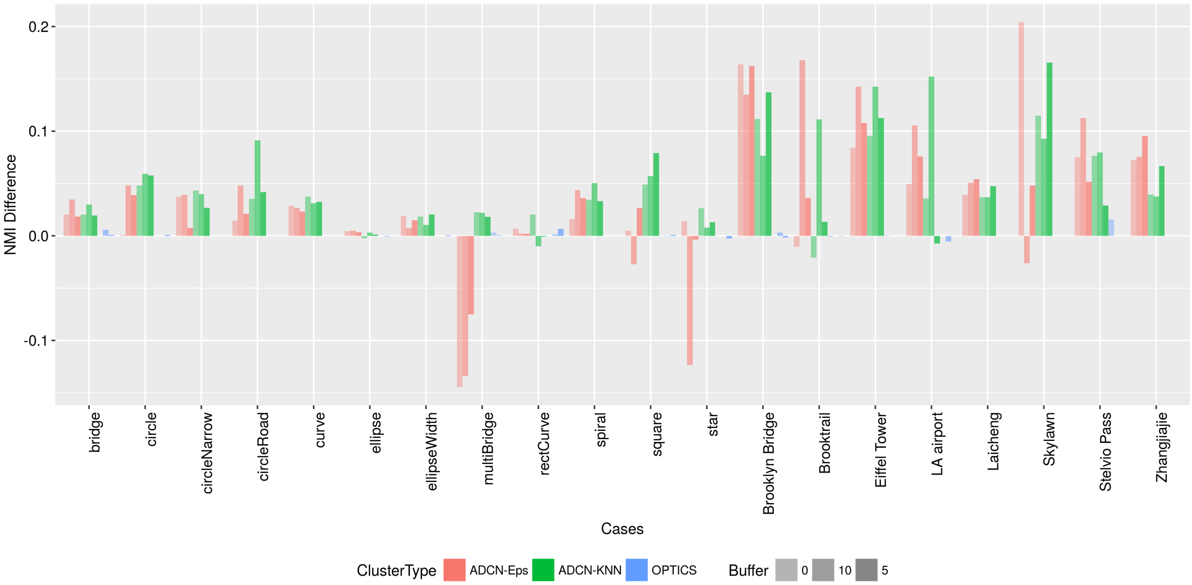

Figure 4.4: Clustering quality comparisons: NMI Difference between 3 clustering methods and DBSCAN for each case. Synthetic cases are on the left, real-world cases on the right.

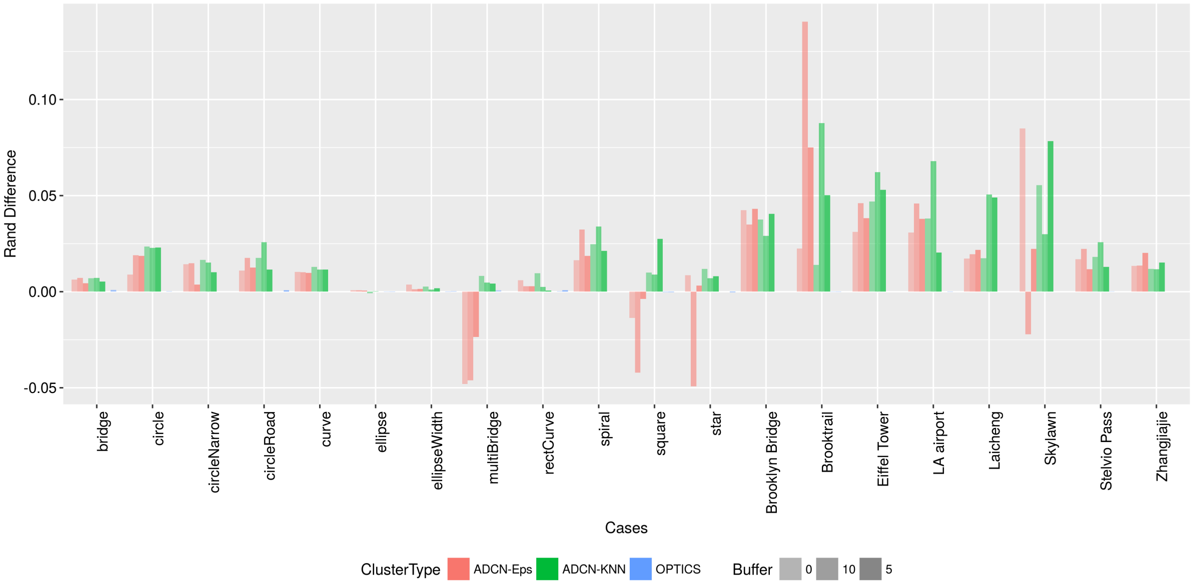

Figure 4.5: Clustering quality comparisons: Rand Difference between 3 clustering methods and DBSCAN for each case. Synthetic cases are on the left, real-world cases on the right.

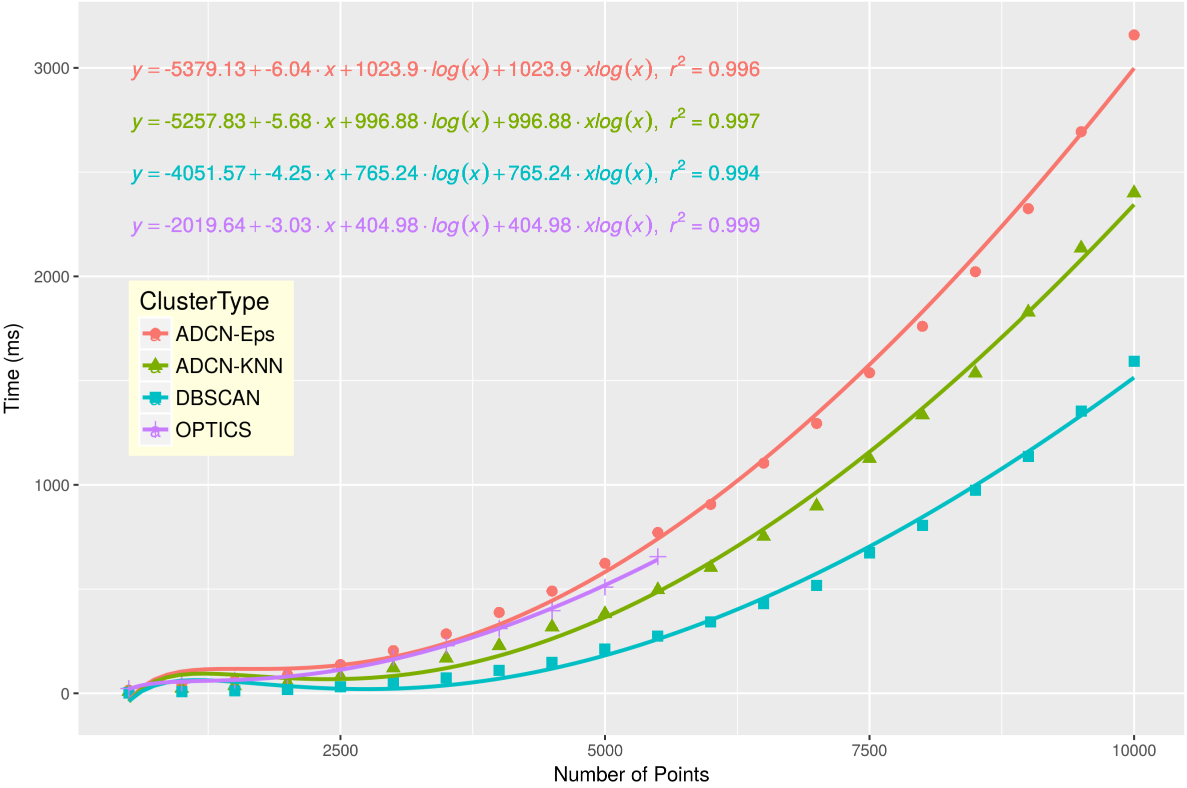

Figure 4.6: Comparison of clustering efficiency with different dataset sizes; runtimes are given in millisecond (The used OPTICS library failed on datasets exceeding 5500 points)

Chapter 5

Real World Application

In this chapter, we will discuss the application of ADCN for the computation of urban areas of interest (AOI) from user-generated geotagged photos collected by the Flickr platform. In Chapter 2 Section 2.1, we already mentioned multiple applications of density-based clustering algorithms. Since ADCN is part of the density-based clustering algorithm family, all the applications we discussed before can also use ADCN instead. Here, our focus is on how the results of ADCN differ from those of DBSCAN for common application examples in GIScience and computer science. Put differently, does the use of ADCN over DBSCAN produce significantly different results when it matters? We will focus on comparison here by relying on previous work as a ground truth for AOI is not available.

In previous work, Hu et al. [2] proposed a framework for extracting urban AOIs from geotagged photos. We will use the same workflow as Hu et al. did except we will apply four different algorithms, namely DBSCAN, OPTICS, ADCN-Eps, and ADCN-KNN, to the geotagged Flickr photos data to extract clusters. By comparing the extracted urban AOIs from different clustering algorithms, we can further understand the performance difference of these algorithms. We will briefly describe the workflow below. Readers with further interests are referred to the original paper [2]. In order to compare our results with that of Hu et al., we use the same datasets as they did which are the Flickr geotagged photos data from six cities including Dubai, London, Mumbai, New York, Paris, Shanghai. We only show the results of 2013-2014 Flickr data here.

5.1 Data Preprocessing and Clustering

The first step is data preprocessing and selection of appropriate *Eps* and *MinPts* for each clustering algorithm. As Hu et al. stated,"Due to the varying numbers of Flickr users and photos in different cities and different years, a single absolute value for *MinPts* may not be suitable. Thus, we handle this variation issue by setting *MinPts* as a percentage of the Flickr users who have visited that city in that year". We did the same thing in this work. The results of the clustering quality evaluation experiments show that the four algorithms, ADCN-Eps, ADCN-KNN, DBSCAN and OPTICS, will not achieve the best clustering results with the same *Eps* and *MinPts.* So we need to identify the proper values of *Eps* and *MinPts* for each algorithm. As for DBSCAN, we use the same parameter combination as Hu et al. which is *Eps* as 200m and *MinPts* as 2%. We use NYC as the reference for parameters' calibration. We stepwise change the parameter combinations with *Eps* from 100m to 500m and *MinPts* from 1% to 5%. In each iteration, we use the value of *Eps* as the search radius to pre-process the data such that each user, i.e., person who took a picture, has one geotagged photo within the search neighborhood. Thereby we reduce the dominance effect of active users which is a common problem in social media. The best parameter combination for each clustering algorithm can be seen in Table 5.1. The best parameter combinations for each clustering algorithms are used to process the 2013-2014 Flickr data of the six cities in our study to retrieve the point clusters. One best clustering result is obtained for each city and each clustering algorithm. In total, we have 24 clustering results.

Table 5.1: The best parameter combinations for four clustering algorithm.

algorithm	Eps	MinPts	λ_p
DBSCAN	200	2%	39
OPTICS	200	2%	41
ADCN-Eps	170	1.7%	34
ADCN-KNN	185	1.7%	29

5.2 Constructing AOI from point clusters using chi-shape algorithm

After 24 clustering results have been identified, areas (polygons) need to be constructed from each cluster of these clustering results. A typical method to approximate such shapes of a point cluster are convex hulls, i.e., finding the minimum bounding *convex polygon* for a set of points which are all within this convex polygon. However, since the clusters identified by four algorithms have arbitrary shapes, using a convex hull to approximate the shape of a point cluster may lead to large empty space which are not occupied by the original point cluster. The *Chi-shape (concave hull)* algorithm [26] is instead used for this step to obtain a better estimation of the shape of each cluster. It first computes a Delaunay triangulation based on the set of point of this cluster whose outer boundary is the convex hull of the point cluster. Then it erodes the convex hull step-by-step until the longest edge of the generated polygon is less than a threshold which is controlled by a normalized length parameter $\lambda_p \in [1, 100]$. A *simple polygon* for each point cluster is derived for each point cluster as the output of *Chi-shape* algorithm.

In order to get an appropriate value for λ_p, the fitness function proposed by Akdag et al. [73] is applied as Equation 5.1:

$$\phi(P, D) = Emptiness(P, D) + C * Complexity(P) \tag{5.1}$$

Here ϕ is the fitness function/score which is used to balance the *complexity* [74] and the *emptiness* of the constructed polygons. P and D represent the derived simple polygon and the Delaunay triangulationof the corresponding point cluster. We use the implementation of fitness function from Hu et al. [1]. The fitness score ϕ is computed per point cluster which is a function of normalized length parameter λ_p. So we iterate λ_p from 1 to 100. For each λ_p, we compute the average fitness score of all point clusters from the six cities for each clustering algorithm. The resulting curves of the average fitness scores for each clustering algorithm are shown in Figure 5.1. Table 5.1 shows the best λ_p for each algorithm.

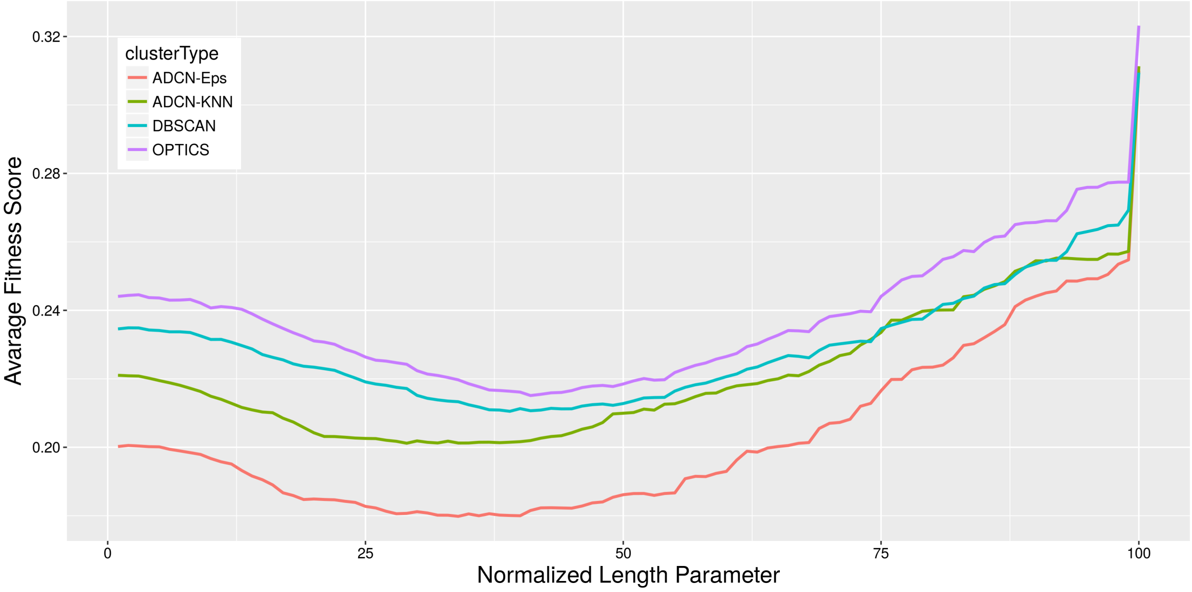

Figure 5.1: Curve plot of the normalized length parameter and the average fitness score.

By using the best λ_p for each clustering algorithm, we construct the urban AOI for

---

[1] `https://github.com/YingjieHu/BalancedConcaveHull`

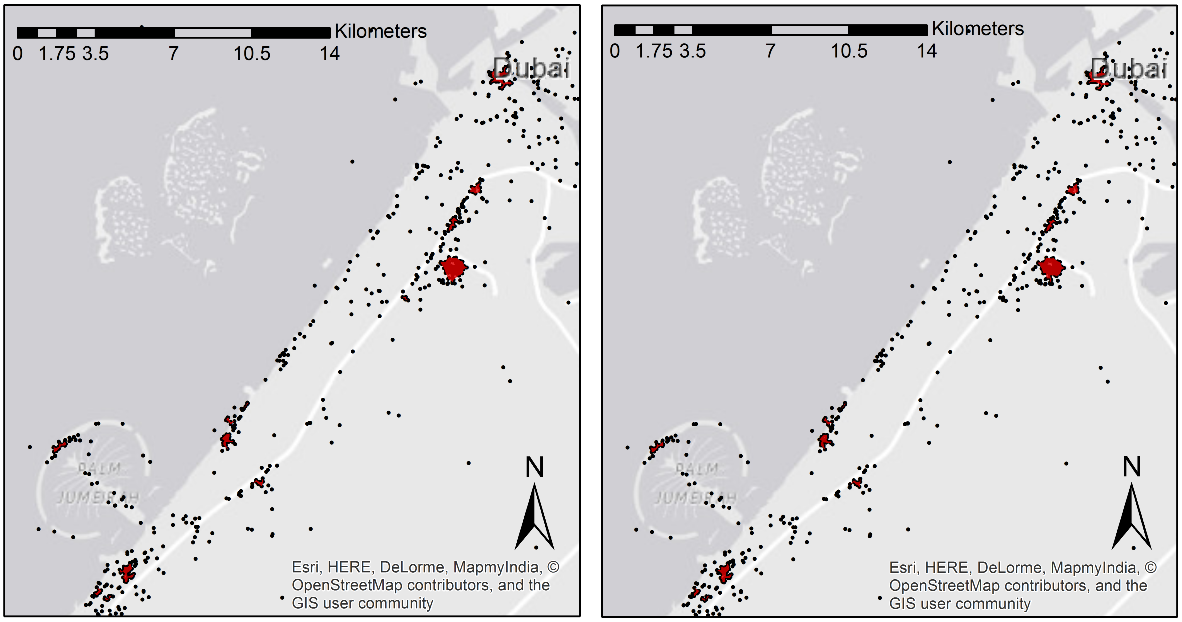
Kilometers
0 1.75 3.5 7 10.5 14
Dubai
PALM JUMEIRAH
N
Esri, HERE, DeLorme, MapmyIndia, © OpenStreetMap contributors, and the GIS user community

DBSCAN **OPTICS**

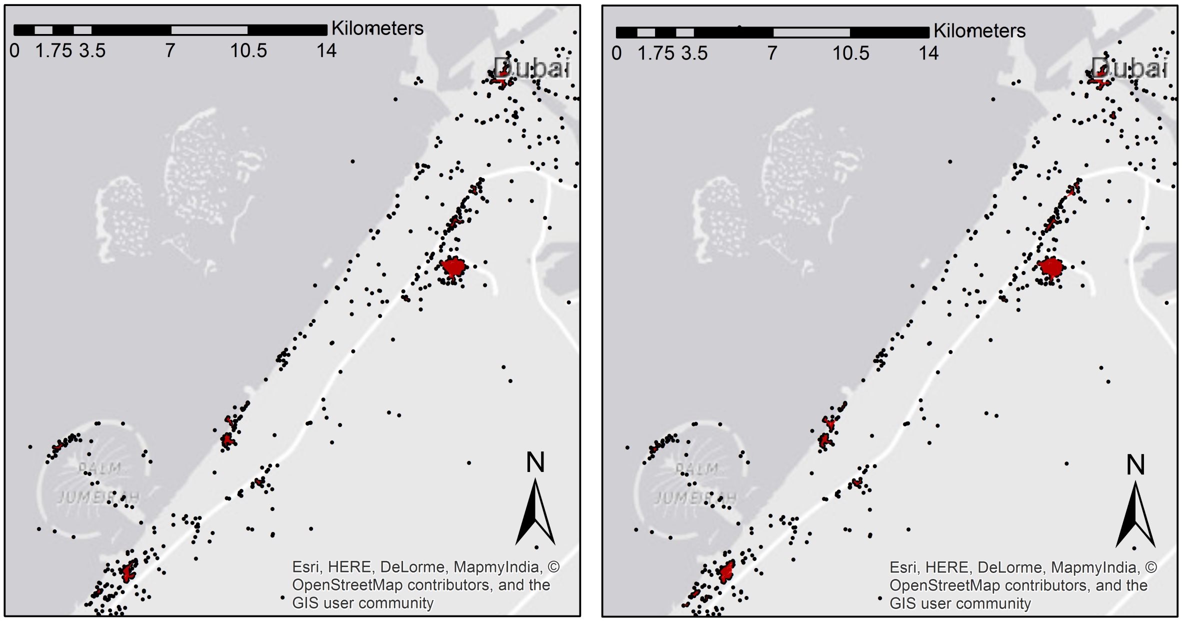
Kilometers
0 1.75 3.5 7 10.5 14
Dubai
PALM JUMEIRAH
N
Esri, HERE, DeLorme, MapmyIndia, © OpenStreetMap contributors, and the GIS user community

ADCN-Eps **ADCN-KNN**

Figure 5.2: Comparison of extracted urban AOI in **Dubai** from four clustering algorithms.

each city and each algorithm. Figure 5.2, 5.3, 5.4, 5.5, 5.6, 5.7 compare the extracted AOIs from different clustering algorithms in these six cities. Some interesting informa-

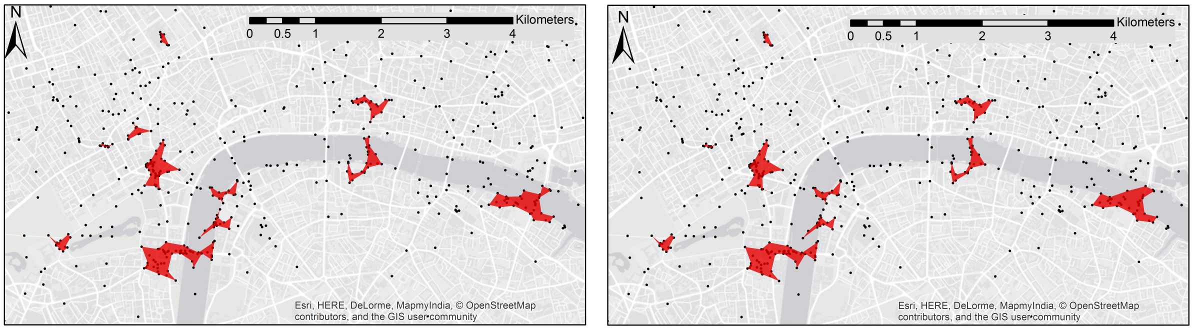
N
Kilometers
0 0.5 1 2 3 4
Esri, HERE, DeLorme, MapmyIndia, © OpenStreetMap contributors, and the GIS user community
N
Kilometers
0 0.5 1 2 3 4
Esri, HERE, DeLorme, MapmyIndia, © OpenStreetMap contributors, and the GIS user community

DBSCAN **OPTICS**

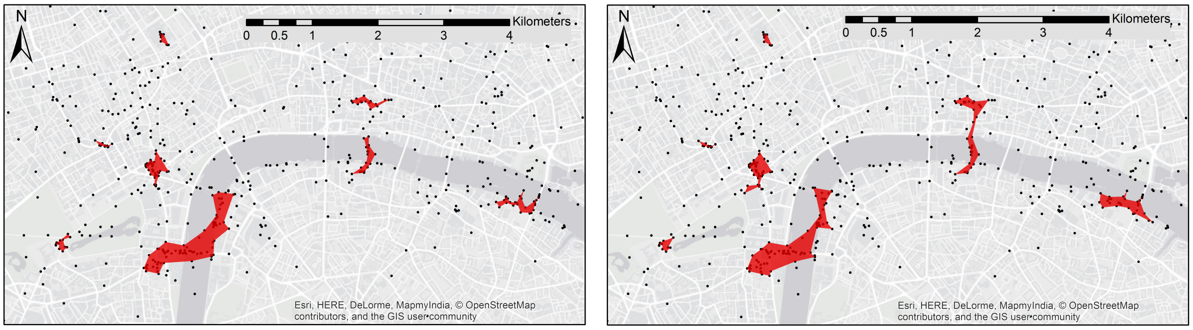
N
Kilometers
0 0.5 1 2 3 4
Esri, HERE, DeLorme, MapmyIndia, © OpenStreetMap contributors, and the GIS user community
N
Kilometers
0 0.5 1 2 3 4
Esri, HERE, DeLorme, MapmyIndia, © OpenStreetMap contributors, and the GIS user community

ADCN-Eps **ADCN-KNN**

Figure 5.3: Comparison of extracted urban AOI in **London** from four clustering algorithms.

tion can be obtained when we compare these AOIs. Since there is no ground truth for urban AOI extraction task, we cannot draw a conclusion about which algorithm is the best for this task. However, a visual comparison among AOIs from different algorithms does help us to understand how different these four algorithms perform on real-world datasets. Here, we select two examples: Brooklyn Bridge in New York and Nanjing Road in Shanghai which are depicted as areas within blue boxes in Figure 5.5 and 5.7. These two areas are further shown in detail in Figure 5.8 and 5.9 [2]. Compared with the AOIs extracted from DBSCAN and OPTICS, AOIs extracted from ADCN are better aligned with the underline road network and ADCN turns out to discover AOIs with linear shapes. For example, In Figure 5.9, the AOIs extracted from Brooklyn Bridge in

---

[2] We change the base map to Openstreet Map with more detail geographic information which can help us to understand the semantic of the extracted AOIs.

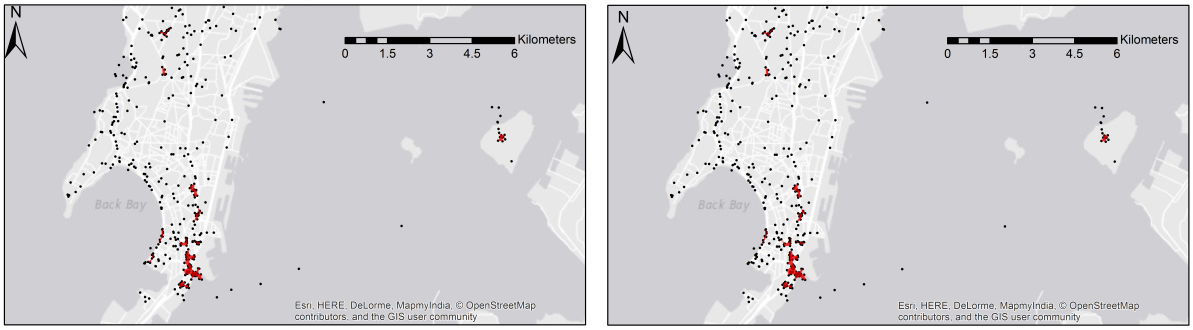
N
Kilometers
0 1.5 3 4.5 6
Back Bay
Esri, HERE, DeLorme, MapmyIndia, © OpenStreetMap contributors, and the GIS user community
N
Kilometers
0 1.5 3 4.5 6
Back Bay
Esri, HERE, DeLorme, MapmyIndia, © OpenStreetMap contributors, and the GIS user community

DBSCAN **OPTICS**

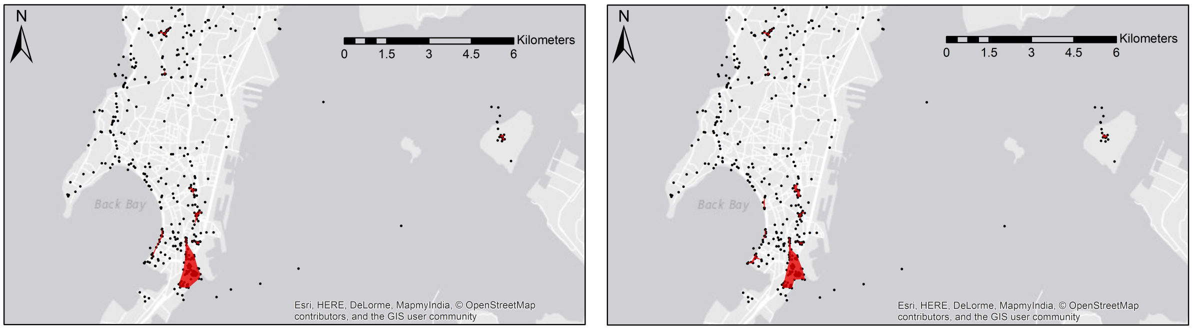
N
Kilometers
0 1.5 3 4.5 6
Back Bay
Esri, HERE, DeLorme, MapmyIndia, © OpenStreetMap contributors, and the GIS user community
N
Kilometers
0 1.5 3 4.5 6
Back Bay
Esri, HERE, DeLorme, MapmyIndia, © OpenStreetMap contributors, and the GIS user community

ADCN-Eps **ADCN-KNN**

Figure 5.4: Comparison of extracted urban AOI in **Mumbai** from four clustering algorithms.

NYC does follow the shape of the bridge while filtering out the Flickr photos on the river (i.e., *noise*). In contrast, the AOIs extracted from DBSCAN and OPTICS for the same area are stretched out because of some geotagged photos located in the river have been included into the clusters. In Figure 5.7, AOIs extracted near Nanjing Road in Shanghai by DBSCAN show two separated areas while ADCN-KNN extracts one linear-shape AOI which follows Nanjing Road.

Through a visual comparison across the AOIs extracted by using the different clustering algorithms, we can draw some interesting conclusions: 1) ADCN is a good alternative of DBSCAN for the Urban AOI Extraction task. The AOIs extracted by ADCN have similar spatial distributions and shapes as those extracted by DBSCAN and OPTICS with an appropriate clustering parameter combination. 2) ADCN tends to connect multiple small clusters which have similar cardinal directions and create a larger cluster

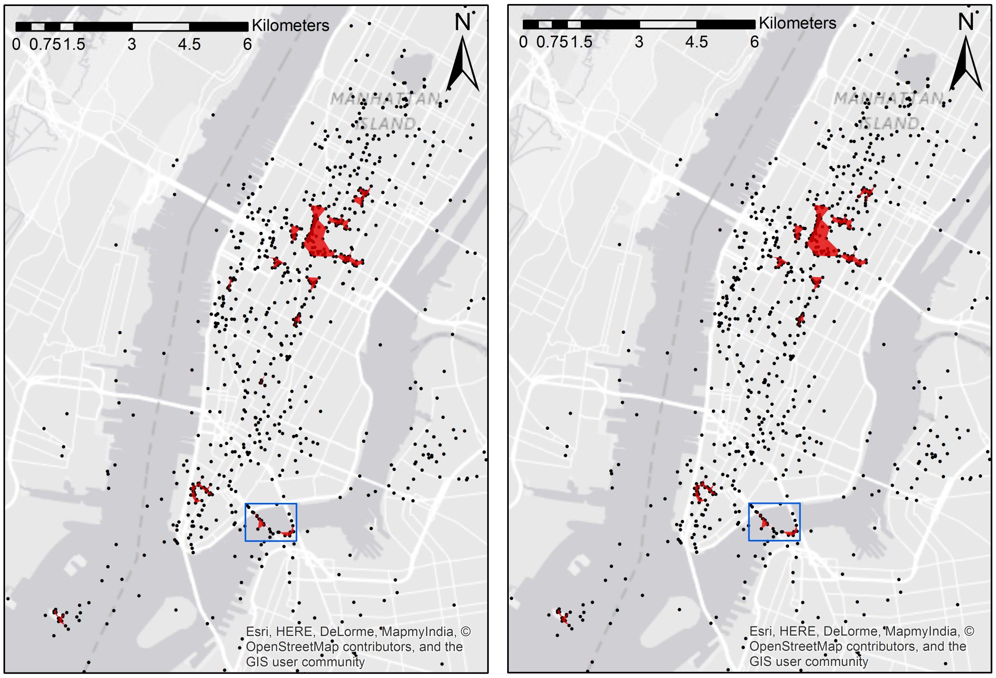
Kilometers
0 0.751.5 3 4.5 6
N
MANHATTAN ISLAND
Esri, HERE, DeLorme, MapmyIndia, © OpenStreetMap contributors, and the GIS user community

DBSCAN **OPTICS**

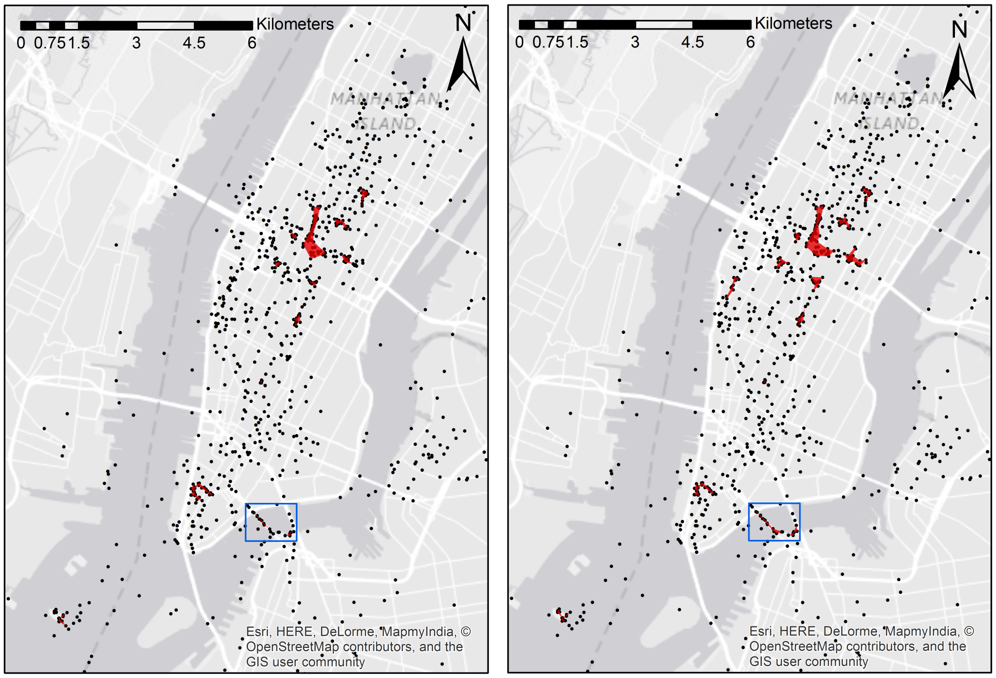
Kilometers
0 0.751.5 3 4.5 6
N
MANHATTAN ISLAND
Esri, HERE, DeLorme, MapmyIndia, © OpenStreetMap contributors, and the GIS user community

ADCN-Eps **ADCN-KNN**

Figure 5.5: Comparison of extracted urban AOI in **New York** from four clustering algorithms.

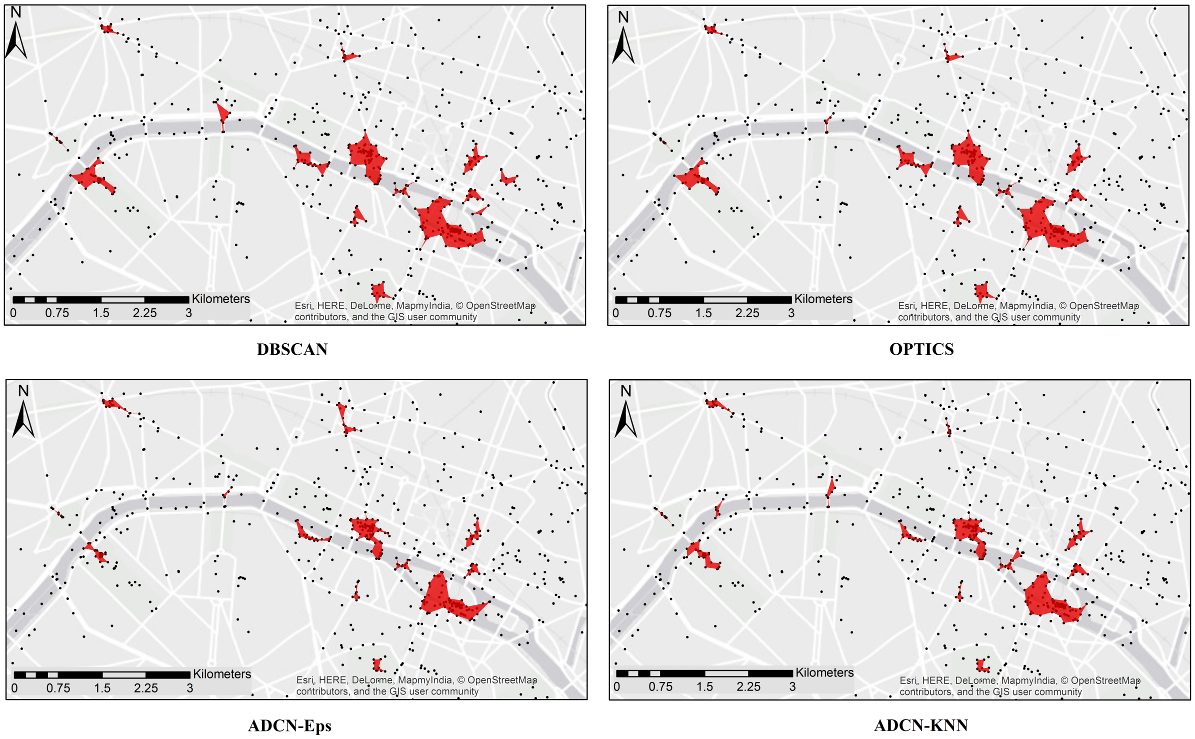
N
Kilometers
0
0.75
1.5
2.25
3
Esri, HERE, DeLorme, MapmyIndia, © OpenStreetMap contributors, and the GIS user community

DBSCAN

OPTICS

ADCN-Eps

ADCN-KNN

Figure 5.6: Comparison of extracted urban AOI in **Paris** from four clustering algorithms.

which follows the underline spatial structures like road networks. 3) ADCN is better at filtering out noise and extracts linear-shape clusters when the points of the clusters follow a similar *local* direction. Summing up, while there is no ground truth for AOI extraction, our comparison shows that ADCN results differ clearly from DBSCAN for areas that show anisotropicity. Put differently, while we established the benefits of using ADCN for synthetic and real-world use cases before, here we showed that these differences are also notable in practical applications.

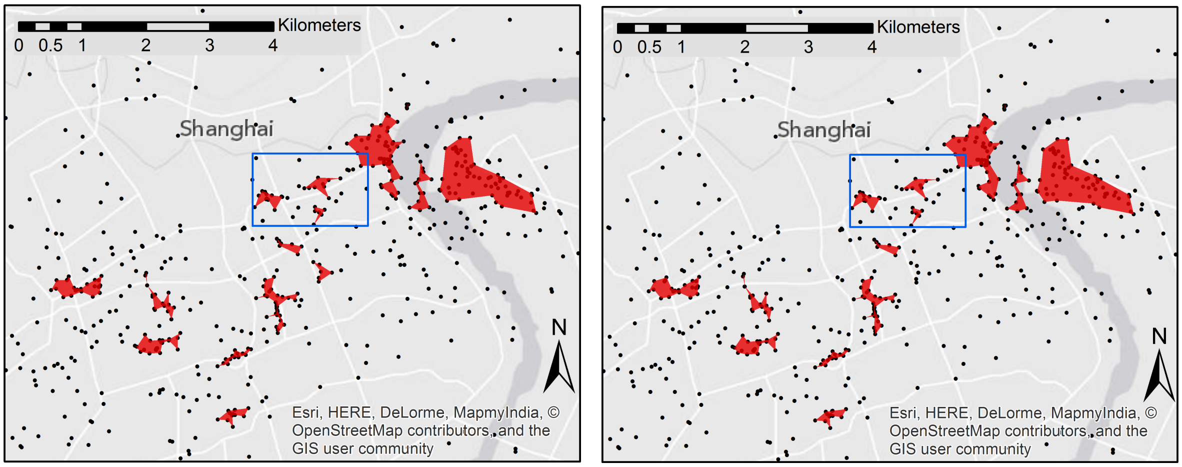
Kilometers
0 0.5 1 2 3 4
Shanghai
N
Esri, HERE, DeLorme, MapmyIndia, © OpenStreetMap contributors, and the GIS user community
Kilometers
0 0.5 1 2 3 4
Shanghai
N
Esri, HERE, DeLorme, MapmyIndia, © OpenStreetMap contributors, and the GIS user community

DBSCAN **OPTICS**

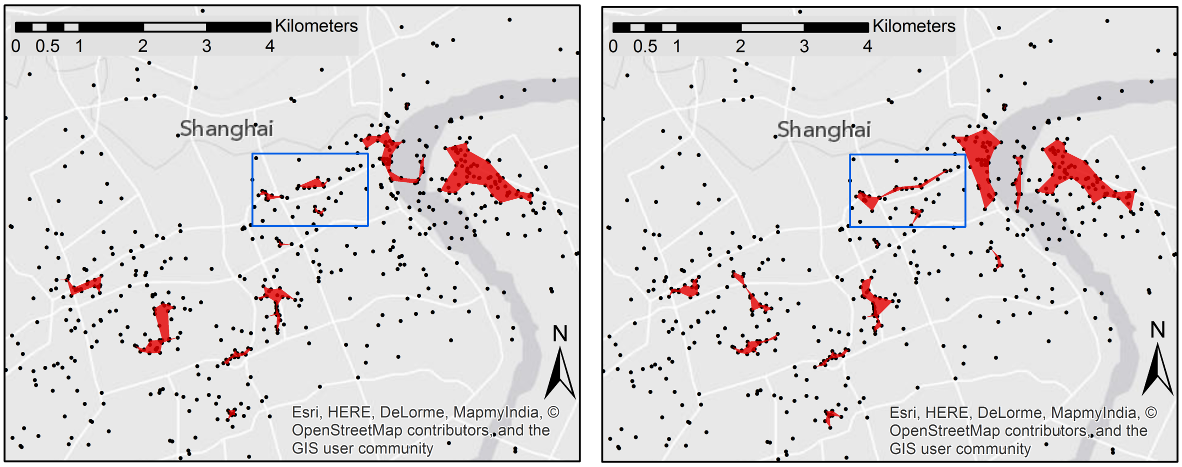
Kilometers
0 0.5 1 2 3 4
Shanghai
N
Esri, HERE, DeLorme, MapmyIndia, © OpenStreetMap contributors, and the GIS user community
Kilometers
0 0.5 1 2 3 4
Shanghai
N
Esri, HERE, DeLorme, MapmyIndia, © OpenStreetMap contributors, and the GIS user community

ADCN-Eps **ADCN-KNN**

Figure 5.7: Comparison of extracted urban AOI in **Shanghai** from four clustering algorithms.

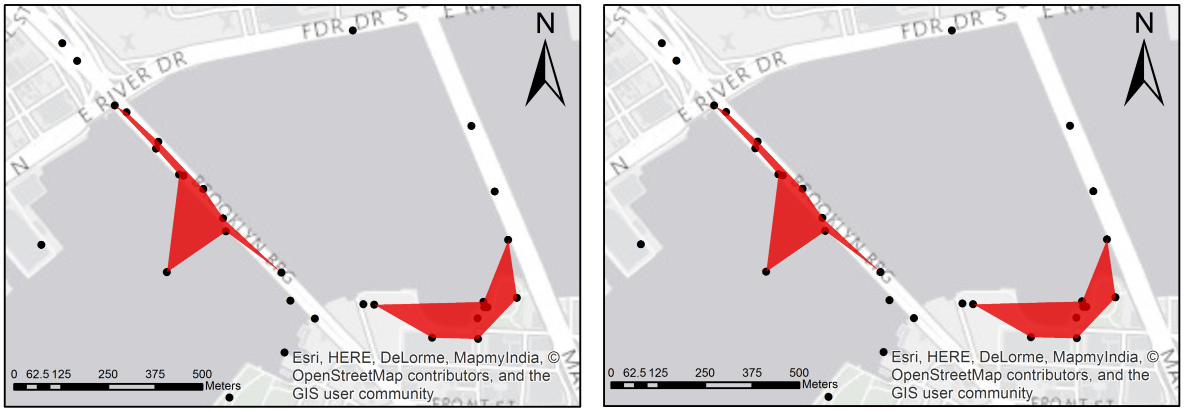
FDR DR S
E RIVER DR
BROOKLYN BRG
N
0 62.5 125 250 375 500
Meters
Esri, HERE, DeLorme, MapmyIndia, © OpenStreetMap contributors, and the GIS user community

DBSCAN **OPTICS**

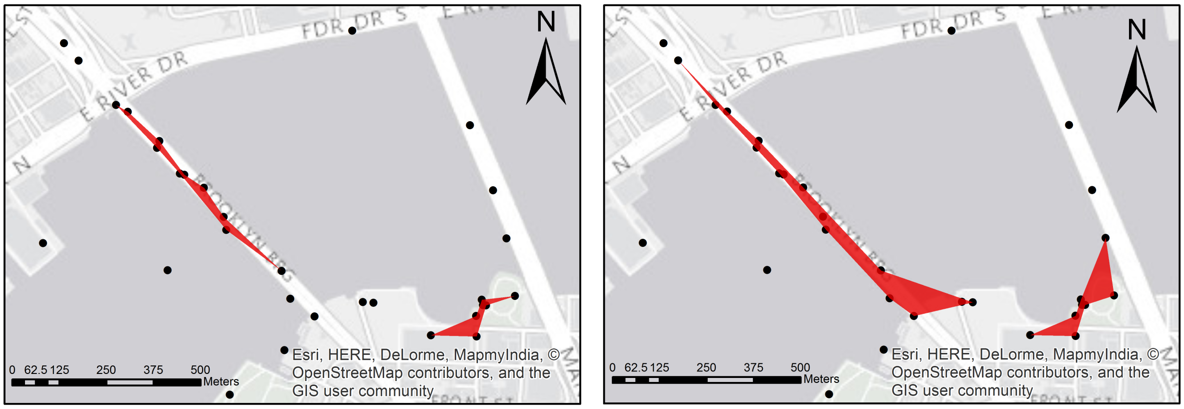
FDR DR S
E RIVER DR
BROOKLYN BRG
N
0 62.5 125 250 375 500
Meters
Esri, HERE, DeLorme, MapmyIndia, © OpenStreetMap contributors, and the GIS user community

ADCN-Eps **ADCN-KNN**

Figure 5.8: Comparison of extracted urban AOI around **Brooklyn Bridge**in **New York** from four clustering algorithms.

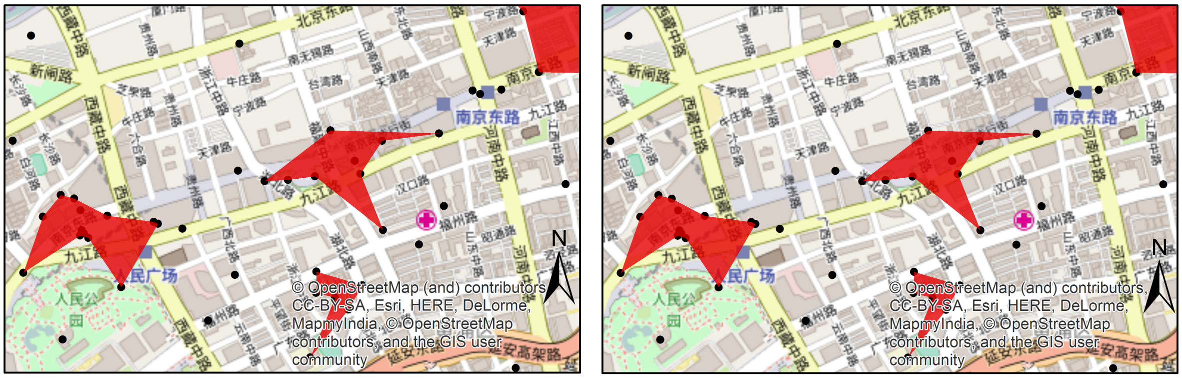
北京东路
南京东路
九江路
西藏中路
人民广场
© OpenStreetMap (and) contributors, CC-BY-SA, Esri, HERE, DeLorme, MapmyIndia, © OpenStreetMap contributors, and the GIS user community
N

DBSCAN **OPTICS**

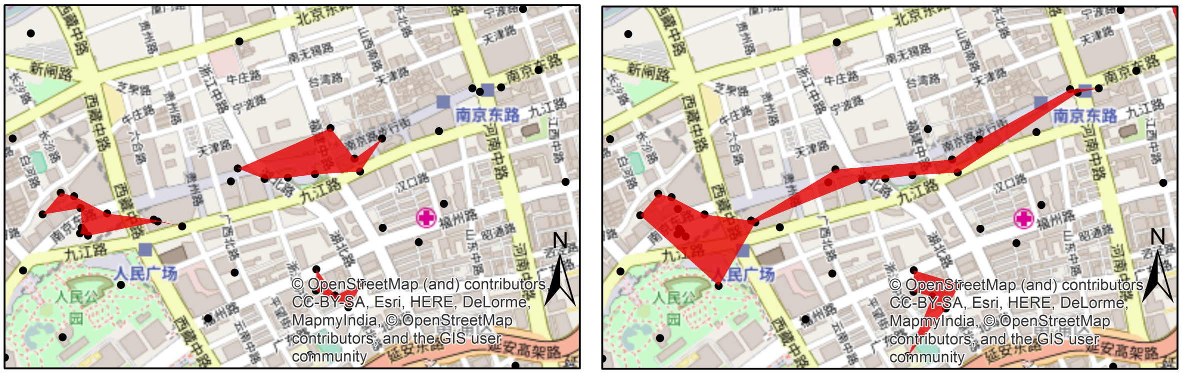
北京东路
南京东路
九江路
西藏中路
人民广场
© OpenStreetMap (and) contributors, CC-BY-SA, Esri, HERE, DeLorme, MapmyIndia, © OpenStreetMap contributors, and the GIS user community
N

ADCN-Eps **ADCN-KNN**

Figure 5.9: Comparison of extracted urban AOI around **Nanjing Road** in **Shanghai** from four clustering algorithms.

Chapter 6

Conclusion and Future Work

In this work, we proposed an anisotropic density-based clustering algorithm (ADCN). We evaluate the clustering quality and clustering efficiency of ADCN to demonstrate the advantages it has over two other density-based clustering algorithms, namely DBSCAN and OPTICS. We then applied ADCN, DBSCAN, and OPTICS to a specific geographic information retrieval and discovery task, namely Urban AOI extraction. By visually comparing the results from different clustering algorithms, we highlighted differences resulting from the usage of ADCN. This chapter summarizes our results of these experiments and discusses future directions for research.

6.1 Conclusion

Density-based clustering algorithm has been widely applied to numerous spatial knowledge discovery tasks. Many of these tasks are aimed at extracting interesting patterns from human mobility or animal trajectories. For example, Huang et al. [29] applied DBSCAN to extract physical activity areas of individuals from sparse footprints accumulated over a long period from geotagged tweets. Damiani et al. [32] used SeqScan, which is similar to ST-DBSCAN, to detect fine-grained movement patterns from the trajectories of roe and red deer. By doing so, an isotropic assumption is accepted implicitly. However, the genesis of many geographic phenomena demonstrates clear *anisotropic* spatial processes. For example, geotagged social media data are following the spatial distribution of transportation networks, trajectories, e.g., of a vessel, building floors, and so forth, because human activity are highly restricted by urban design and topography. That means if we apply clustering algorithms which take an isotropic assumption like DBSCAN to these kind of data, it is possible that the clustering algorithms will segment a single line-segment shaped cluster into multiple circle-shape clusters. Hence an anisotropic version of DBSCAN is desirable. Hence, in this work we developed and tested an anisotropic density-based clustering algorithm (ADCN).

Both synthetic and real-world cases have been used to verify the clustering quality and efficiency of our algorithm compared to DBSCAN and OPTICS. As for the clustering quality evaluation, two clustering quality evaluation metrics have been used to compare the clustering results with the *ground truth*, namely Normalized Mutual Information and Rand Index. We demonstrate that ADCN-KNN outperforms DBSCAN and OPTICS for the detection of anisotropic spatial point patterns and performs equally well in cases that do not explicitly benefit from an anisotropic perspective. As for the clustering efficiency evaluation, we implement two versions of each clustering algorithm, one with a R-tree spatial index and one without any spatial indexes. And we show that ADCN has the same time complexity as DBSCAN and OPTICS, namely O(n log n) when using a spatial index and O(n^2) otherwise. With respect to the average runtime, the performance of ADCN is comparable to OPTICS.

Our algorithm as well as DBSCAN and OPTICS are further applied to the task of Urban AOI Extraction task. We follow the same workflow as Hu et al. did [2] and use the same dataset to extract AOIs from Flickr geotagged photos. The only difference is that we use those four clustering algorithms for clustering instead of just DBSCAN. Since different clustering algorithms achieve their optimal performance with different clustering parameter combinations, we selected the appropriate clustering parameter combinations for each clustering algorithm. After detecting the point clusters, *chi-shape* has been applied to construct concave hulls of all clusters. During the concave hull construction process, we used a fitness function (See Equ. 5.1) to select the optimal λ_p for each clustering algorithms. Visual comparison among the urban AOI derived from different clustering algorithms shows that ADCN is a good alternative of DBSCAN for Urban AOI extraction. It tends to extract linear-shaped AOIs and connects areas when the spatial distribution of these areas show similar directional trends.

6.2 Future Work

From the clustering evaluation, we can clearly see that ADCN has a better performance than DBSCAN and OPTICS when the spatial data shows a clear *anisotropic* trend. As geospatial data is often generated from *anisotropic* spatial processes, we can see a wide range of application areas for this algorithm. They include (but are not limited to) cleaning and clustering geotagged social media data, e.g., from Twitter, Flickr or Strava, and analyzing trajectories collected from car sensors, wildlife tracking, and so forth. The Urban AOI extraction is one such application example.

As with other clustering techniques, an important and challenging question for ADCN and other density-based clustering algorithms is how to derive an optimal parameter combination (Eps, $MinPts$) given a specific spatial knowledge discovery task and a specific dataset. In this work, we stepwise tried every possible parameter combinations computationally. In each iteration, we used two clustering quality metrics, NMI and Rand Index, to compare the results from the clustering algorithm with the *ground truth*.

The best parameter combination is determined by finding the highest NMI or Rand Index. This is called an *extrinsic* evaluation method. It will fail if the *ground truth* is not available which is usually the case. This problem is not specific to ADCN but many other clustering techniques as well. In fact, the Urban AOI extraction task well demonstrates this problem. Using samples for ground truthing is a common approach but other methods should be studied in the future.

There are also some *intrinsic* methods which do not use *ground truth* to evaluate clustering results, like Silhouette [75] which is usually used to determine the number of clusters in data sets [76]. The basic idea behind Silhouette is that they evaluate how well two clusters are separated from each other. The closer each point of clusters is to their own cluster prototype point and the further each cluster is to each other, the better the clustering result is. We can see that Silhouette does not consider the density information and direction information in the clustering evaluation process which is not true for human interpretation of the clustering results. So in order to have an intrinsic measure of the clustering quality, we need to study the cognition aspects of clustering. That means we need to better understand how humans interpret the direction and density information in a spatial point data set and how humans perform noise detection task visually.

Bibliography

[1] S. Gao, L. Li, W. Li, K. Janowicz, and Y. Zhang, *Constructing gazetteers from volunteered big geo-data based on hadoop*, *Computers, Environment and Urban Systems* **61** (2017) 172–186.

[2] Y. Hu, S. Gao, K. Janowicz, B. Yu, W. Li, and S. Prasad, *Extracting and understanding urban areas of interest using geotagged photos*, *Computers, Environment and Urban Systems* **54** (2015) 240–254.

[3] S. Gao, K. Janowicz, D. R. Montello, Y. Hu, J.-A. Yang, G. McKenzie, Y. Ju, L. Gong, B. Adams, and B. Yan, *A data-synthesis-driven method for detecting and extracting vague cognitive regions*, *International Journal of Geographical Information Science* **31** (2017), no. 6 1245–1271.

[4] Q. Huang, G. Cao, and C. Wang, *From where do tweets originate?: a gis approach for user location inference*, in *Proceedings of the 7th ACM SIGSPATIAL International Workshop on Location-Based Social Networks*, pp. 1–8, ACM, 2014.

[5] S. Jiang, J. Ferreira, and M. C. González, *Clustering daily patterns of human activities in the city*, *Data Mining and Knowledge Discovery* (2012) 1–33.

[6] S. I. Fabrikant, D. Monteilo, and D. M. Mark, *The distance-similarity metaphor in region-display spatializations*, *IEEE Computer Graphics and Applications* **26** (2006), no. 4 34–44.

[7] S. I. Fabrikant and D. R. Montello, *The effect of instructions on distance and similarity judgements in information spatializations*, *International Journal of Geographical Information Science* **22** (2008), no. 4 463–478.

[8] M. Ester, H.-P. Kriegel, J. Sander, and X. Xu, *A density-based algorithm for discovering clusters in large spatial databases with noise.*, in *Proceedings of 2nd International Conference on KDD*, vol. 96, pp. 226–231, 1996.

[9] M. Ankerst, M. M. Breunig, H.-P. Kriegel, and J. Sander, *OPTICS: ordering points to identify the clustering structure*, in *Proceedings of ACM SIGMOD Conference*, vol. 28, pp. 49–60, ACM, 1999.

[10] J. MacQueen *et. al.*, *Some methods for classification and analysis of multivariate observations*, in *Proceedings of the fifth Berkeley symposium on mathematical statistics and probability*, vol. 1, pp. 281–297, Oakland, CA, USA., 1967.

[11] A. K. Jain and R. C. Dubes, *Algorithms for clustering data.* Prentice-Hall, Inc., 1988.

[12] M. Deng, Q. Liu, T. Cheng, and Y. Shi, *An adaptive spatial clustering algorithm based on delaunay triangulation*, *Computers, Environment and Urban Systems* **35** (2011), no. 4 320–332.

[13] D. Comaniciu and P. Meer, *Mean shift: A robust approach toward feature space analysis*, *IEEE Transactions on Pattern Analysis and Machine Intelligence* **24** (2002), no. 5 603–619.

[14] D. L. Davies and D. W. Bouldin, *A cluster separation measure*, *IEEE Transactions on Pattern Analysis and Machine Intelligence* (1979), no. 2 224–227.

[15] E. Hoek, *Fracture of anisotropic rock*, *Journal of the South African Institute of Mining and Metallurgy* **64** (1964), no. 10 501–523.

[16] L. Barden, *Stresses and displacements in a cross-anisotropic soil*, *Geotechnique* **13** (1963), no. 3 198–210.

[17] E. H. Isaaks and R. M. Srivastava, *Applied geostatistics*, .

[18] M.-j. Fortin, M. R. Dale, and J. M. Ver Hoef, *Spatial analysis in ecology*, *Encyclopedia of environmetrics* (2002).

[19] G. Mai, K. Janowicz, Y. Hu, and S. Gao, *Adcn: an anisotropic density-based clustering algorithm*, in *Proceedings of the 24th ACM SIGSPATIAL International Conference on Advances in Geographic Information Systems*, p. 58, ACM, 2016.

[20] G. Mai, K. Janowicz, Y. Hu, and S. Gao, *Adcn: An anisotropic density-based clustering algorithm for discovering spatial point patterns with noise*, *Transaction in GIS* (in press).

[21] J. Han, J. Pei, and M. Kamber, *Data mining: concepts and techniques.* Elsevier, 2011.

[22] L. Kaufman and P. J. Rousseeuw, *Finding groups in data: an introduction to cluster analysis*, vol. 344. John Wiley & Sons, 2009.

[23] R. T. Ng and J. Han, *Clarans: A method for clustering objects for spatial data mining*, *IEEE transactions on knowledge and data engineering* **14** (2002), no. 5 1003–1016.

[24] C.-F. Tsai and C.-W. Liu, *KIDBSCAN: a new efficient data clustering algorithm*, in *International Conference on Artificial Intelligence and Soft Computing*, pp. 702–711, Springer, 2006.

[25] A. Moreira and M. Y. Santos, *Concave hull: A k-nearest neighbours approach for the computation of the region occupied by a set of points*, in *Proceedings of the International Conference on Computer Graphics Theory and Applications*, pp. 61–68, 2007.

[26] M. Duckham, L. Kulik, M. Worboys, and A. Galton, *Efficient generation of simple polygons for characterizing the shape of a set of points in the plane*, *Pattern Recognition* **41** (2008), no. 10 3224–3236.

[27] X. Zhong and M. Duckham, *Characterizing the shapes of noisy, non-uniform, and disconnected point clusters in the plane*, *Computers, Environment and Urban Systems* **57** (2016) 48–58.

[28] Q. Huang and D. W. Wong, *Modeling and visualizing regular human mobility patterns with uncertainty: an example using twitter data*, *Annals of the Association of American Geographers* **105** (2015), no. 6 1179–1197.

[29] Q. Huang, *Mining online footprints to predict users next location*, *International Journal of Geographical Information Science* **31** (2017), no. 3 523–541.

[30] Q. Huang and D. W. Wong, *Activity patterns, socioeconomic status and urban spatial structure: what can social media data tell us?*, *International Journal of Geographical Information Science* **30** (2016), no. 9 1873–1898.

[31] R. Jurdak, K. Zhao, J. Liu, M. AbouJaoude, M. Cameron, and D. Newth, *Understanding human mobility from twitter*, *PloS one* **10** (2015), no. 7 e0131469.

[32] M. L. Damiani, H. Issa, G. Fotino, M. Heurich, and F. Cagnacci, *Introducing presenceand stationarity indexto study partial migration patterns: an application of a spatio-temporal clustering technique*, *International Journal of Geographical Information Science* **30** (2016), no. 5 907–928.

[33] A. Hinneburg, D. A. Keim, *et. al.*, *An efficient approach to clustering in large multimedia databases with noise*, in *KDD*, vol. 98, pp. 58–65, 1998.

[34] P. Liu, D. Zhou, and N. Wu, *VDBSCAN: varied density based spatial clustering of applications with noise*, in *2007 International conference on service systems and service management*, pp. 1–4, IEEE, 2007.

[35] D. Birant and A. Kut, *ST-DBSCAN: An algorithm for clustering spatial–temporal data*, *Data & Knowledge Engineering* **60** (2007), no. 1 208–221.

[36] J. Sander, M. Ester, H.-P. Kriegel, and X. Xu, *Density-based clustering in spatial databases: The algorithm GDBSCAN and its applications*, *Data mining and knowledge discovery* **2** (1998), no. 2 169–194.

[37] E. Stefanakis, *NET-DBSCAN: clustering the nodes of a dynamic linear network*, *International Journal of Geographical Information Science* **21** (2007), no. 4 427–442.

[38] B. Borah and D. Bhattacharyya, *An improved sampling-based DBSCAN for large spatial databases*, in *Proceedings of International Conference on Intelligent Sensing and Information*, pp. 92–96, IEEE, 2004.

[39] W. Zhou, H. Xiong, Y. Ge, J. Yu, H. T. Ozdemir, and K. C. Lee, *Direction clustering for characterizing movement patterns.*, in *IRI*, pp. 165–170, 2010.

[40] J. Wang and X. Wang, *A spatial clustering method for points-with-directions*, in *Rough Sets and Knowledge Technology*, pp. 194–199. Springer, 2012.

[41] J. A. M. Rocha, V. C. Times, G. Oliveira, L. O. Alvares, and V. Bogorny, *DB-SMoT: A direction-based spatio-temporal clustering method*, in *2010 5th IEEE International Conference Intelligent Systems*, pp. 114–119, IEEE, 2010.

[42] C. B. t. Stroet and J. J. Snepvangers, *Mapping curvilinear structures with local anisotropy kriging*, *Mathematical geology* **37** (2005), no. 6 635–649.

[43] D. F. Machuca-Mory and C. V. Deutsch, *Non-stationary geostatistical modeling based on distance weighted statistics and distributions*, *Mathematical Geosciences* **45** (2013), no. 1 31–48.

[44] J. Boisvert, J. Manchuk, and C. Deutsch, *Kriging in the presence of locally varying anisotropy using non-euclidean distances*, *Mathematical Geosciences* **41** (2009), no. 5 585–601.

[45] R. DErcole and J. Mateu, *On wavelet-based energy densities for spatial point processes*, *Stochastic environmental research and risk assessment* **27** (2013), no. 6 1507–1523.

[46] T. A. Rajala, A. Särkkä, C. Redenbach, and M. Sormani, *Estimating geometric anisotropy in spatial point patterns*, *Spatial Statistics* **15** (2016) 100–114.

[47] J. Møller and H. Toftaker, *Geometric anisotropic spatial point pattern analysis and cox processes*, *Scandinavian Journal of Statistics* **41** (2014), no. 2 414–435.

[48] G. Zhao, T. Wang, and J. Ye, *Anisotropic clustering on surfaces for crack extraction*, *Machine Vision and Applications* **26** (2015), no. 5 675–688.

[49] D. Hanwell and M. Mirmehdi, *QUAC: Quick unsupervised anisotropic clustering*, *Pattern Recognition* **47** (2014), no. 1 427–440.

[50] E. Amigó, J. Gonzalo, J. Artiles, and F. Verdejo, *A comparison of extrinsic clustering evaluation metrics based on formal constraints*, *Information retrieval* **12** (2009), no. 4 461–486.

[51] M. Meilă, *Comparing clusterings by the variation of information*, in *Learning theory and kernel machines*, pp. 173–187. Springer, 2003.

[52] N. X. Vinh, J. Epps, and J. Bailey, *Information theoretic measures for clusterings comparison: Variants, properties, normalization and correction for chance*, *Journal of Machine Learning Research* **11** (2010), no. Oct 2837–2854.

[53] E. Bae, J. Bailey, and G. Dong, *Clustering similarity comparison using density profiles*, in *Australasian Joint Conference on Artificial Intelligence*, pp. 342–351, Springer, 2006.

[54] D. Zhou, J. Li, and H. Zha, *A new mallows distance based metric for comparing clusterings*, in *Proceedings of the 22nd international conference on Machine learning*, pp. 1028–1035, ACM, 2005.

[55] M. H. Coen, M. H. Ansari, and N. Fillmore, *Comparing clusterings in space*, in *Proceedings of the 27th International Conference on Machine Learning (ICML-10)*, pp. 231–238, 2010.

[56] D. L. Wallace, *Comment*, *Journal of the American Statistical Association* **78** (1983), no. 383 569–576.

[57] E. B. Fowlkes and C. L. Mallows, *A method for comparing two hierarchical clusterings*, *Journal of the American statistical association* **78** (1983), no. 383 553–569.

[58] W. M. Rand, *Objective criteria for the evaluation of clustering methods*, *Journal of the American Statistical association* **66** (1971), no. 336 846–850.

[59] L. Hubert and P. Arabie, *Comparing partitions*, *Journal of classification* **2** (1985), no. 1 193–218.

[60] A. Ben-Hur, A. Elisseeff, and I. Guyon, *A stability based method for discovering structure in clustered data*, in *Pacific symposium on biocomputing*, vol. 7, pp. 6–17, 2001.

[61] K. Higbee, *Mathematical classification and clustering*, 1998.

[62] M. Meilă and D. Heckerman, *An experimental comparison of model-based clustering methods*, *Machine learning* **42** (2001), no. 1-2 9–29.

[63] B. Larsen and C. Aone, *Fast and effective text mining using linear-time document clustering*, in *Proceedings of the fifth ACM SIGKDD international conference on Knowledge discovery and data mining*, pp. 16–22, ACM, 1999.

[64] S. van Dongen, *Performance criteria for graph clustering and markov cluster experiments*, .

[65] A. Banerjee, I. S. Dhillon, J. Ghosh, and S. Sra, *Clustering on the unit hypersphere using von mises-fisher distributions*, *Journal of Machine Learning Research* **6** (2005), no. Sep 1345–1382.

[66] Y. Yao, *Information-theoretic measures for knowledge discovery and data mining*, in *Entropy Measures, Maximum Entropy Principle and Emerging Applications*, pp. 115–136. Springer, 2003.

[67] A. Strehl and J. Ghosh, *Cluster ensembles—a knowledge reuse framework for combining multiple partitions*, *Journal of machine learning research* **3** (2002), no. Dec 583–617.

[68] T. O. Kvalseth, *Entropy and correlation: Some comments*, *IEEE Transactions on Systems, Man, and Cybernetics* **17** (1987), no. 3 517–519.

[69] Z. Liu, Z. Guo, and M. Tan, *Constructing tumor progression pathways and biomarker discovery with fuzzy kernel kmeans and dna methylation data*, *Cancer informatics* **6** (2008) 1.

[70] A. Kraskov, H. Stögbauer, R. G. Andrzejak, and P. Grassberger, *Hierarchical clustering using mutual information*, *EPL (Europhysics Letters)* **70** (2005), no. 2 278.

[71] R. S. Yuill, *The standard deviational ellipse; an updated tool for spatial description*, *Geografiska Annaler. Series B, Human Geography* **53** (1971), no. 1 28–39.

[72] M. G. Wing, A. Eklund, and L. D. Kellogg, *Consumer-grade global positioning system (gps) accuracy and reliability*, *Journal of forestry* **103** (2005), no. 4 169–173.

[73] F. Akdag, C. F. Eick, and G. Chen, *Creating polygon models for spatial clusters*, in *International Symposium on Methodologies for Intelligent Systems*, pp. 493–499, Springer, 2014.

[74] T. Brinkhoff, H.-P. Kriegel, R. Schneider, and A. Braun, *Measuring the complexity of polygonal objects.*, in *ACM-GIS*, p. 109, 1995.

[75] P. J. Rousseeuw, *Silhouettes: a graphical aid to the interpretation and validation of cluster analysis*, *Journal of computational and applied mathematics* **20** (1987) 53–65.

[76] R. C. de Amorim and C. Hennig, *Recovering the number of clusters in data sets with noise features using feature rescaling factors*, *Information Sciences* **324** (2015) 126–145.